X-525-68-139

NASA TM X- 63360

EXPERIMENTAL INVESTIGATION OF AN ADAPTIVELY PHASED LARGE APERTURE ARRAY AT VHF

LEONARD F. DEERKOSKI

JULY 1968

GSFC
GODDARD SPACE FLIGHT CENTER
GREENBELT, MARYLAND

X-525-68-139

EXPERIMENTAL INVESTIGATION OF AN ADAPTIVELY PHASED LARGE APERTURE ARRAY AT VHF

Leonard F. Deerkoski

July 1968

GODDARD SPACE FLIGHT CENTER
Greenbelt, Maryland

EXPERIMENTAL INVESTIGATION OF AN ADAPTIVELY PHASED LARGE APERTURE ARRAY AT VHF

Leonard F. Deerkoski

ABSTRACT

A two element adaptively phased array operating at 136 MHz and using the APDAR receiver as the coherent combiner is evaluated. The measured SNR improvement capability of this space diversity system during active satellite experiments is presented. The measured relative phase between the antennas and representative spectra of these data are also given.

CONTENTS

ILLUSTRATIONS

ILLUSTRATIONS (Continued)

TABLES

GLOSSARY OF NOTATION

Symbol	Meaning
SNR	signal-to-noise power ratio
SNR_1, SNR_2	signal-to-noise power ratio in channel one, channel two
SNR_i, SNR_0	input and output signal-to-noise power ratio for a bandpass limiter
F_0	carrier frequency in hertz (cycles per second)
F_1, F_2, F_d	doppler frequency in hertz
f	modulating frequency in hertz
S	signal power level
N	noise power level
C	velocity of light in meters per second
D	antenna separation in meters
T	time delay in seconds
τ_0	fixed time delay of 90.9 nanoseconds
A_1, A_2	peak voltage levels determined by VCO outputs in channel one and channel two
S_1 (40 MHz)	nominal 40 MHz L.O. (local oscillator) used in the channel one mixing stage
S_2 (40 MHz)	nominal 40 MHz L.O. used in the channel two mixing stage
Σ_c, Σ_1, Σ_2	combined output channel, channel one input, channel two input
α, β, γ	space angles in radians
ϕ, θ_1, θ_2, ψ	phase angles in radians
R_1, R_2, R_3	space dimensions in meters
v_r, v_1, v_2	relative velocities in meters per second

EXPERIMENTAL INVESTIGATION OF AN ADAPTIVELY PHASED LARGE APERTURE ARRAY AT VHF

INTRODUCTION

The achievement of high gain receiving capability by a single aperture antenna is limited by both engineering and economic considerations. The required pointing accuracy of antennas in excess of 200 feet in diameter with hemispherical coverage place stringent demands on the servo control system. Surface tolerances on the dish face make the maximum antenna size inversely related to operating frequencies.[1] At the same time, the antenna cost per unit effective area[2] is related to the antenna diameter by $D^{2.94}$ while the gain of the antenna is related by $D^{2.0}$, making each additional square foot more costly. Reflector antennas require a planar phase front across their aperture and phase front distortion on the received signal due to ionospheric and tropospheric disturbances reduces the degree to which the theoretical gain capability of an antenna can be achieved in larger structures.

Each of the problems listed above can be substantially reduced by replacing the single large antenna with an array of antennas of convenient size for the frequencies of interest. When the array elements are properly combined, a maximum theoretical SNR improvement of 3.0 dB over that of the input channels will result each time the number of identical elements is doubled. With the antennas comprising the major cost contribution of the system, the 3.0 dB SNR improvement indicates a linear relationship between cost and array gain. The degree to which the theoretical gain can be achieved will depend on the receiving system and the combining technique used. The major combining techniques have been thoroughly studied[3] and coherent predetection combining with SNR weighting has been found best.

A four element adaptively phased array has already been built and tested by Ohio State University[4] and their results have been favorable. The work in this area has not given SNR improvement characteristics during active satellite passes in sufficient detail to permit the construction of an array of significant size. The program described in this report is the first stage of a study designed to answer

---

[1]Reference 1, p. 50
[2]Reference 1, p. 11
[3]Reference 2
[4]Reference 3

the questions still outstanding on gain improvement capability. In addition, phase front characteristics of signals received from space have been investigated to determine atmospheric distortion effects and the added phasing requirements placed on the receiver by them.

This report has been organized in such a way as to give a complete description of the system and measuring techniques before any results are given. The data presented and analyzed later in the document then permit a more realistic evaluation by the reader in light of the system employed. The APDAR receiver was used as the combiner in the program and the results are therefore biased by the characteristics of this instrument. The VHF portion of the antenna combining study was intended to detail the shortcomings and added requirements of the system not originally anticipated. This information would then be used to modify and update the system to permit improved performance at the S-band stage of the program.

RECEIVING SYSTEM

Antennas

The VHF program utilized a two-element array. The antennas themselves were arrays of five Yagi elements as in Figure 1, each with an equivalent aperture of 15 feet. The antennas were connected for RHC polarization in all cases and provided a nominal gain of 18 dB. The Yagi arrays provided three channel monopulse output for tracking purposes and were mounted on EL/AZ tracking pedestals. The master antenna was fixed to a permanent foundation and was positioned in the auto-track mode by the receiver error signals. The error signals for this program were derived from the master antenna only. The slave antenna was mounted on a trailer (Figure 2) to permit changes in antenna separation. The slave antenna pointing was locked to that of the master antenna.

The program was performed at the Goddard Space Flight Center Antenna Combining Range, located within the boundaries of the Goddard Optical Site. The facility consists of four cement pads defining an array baseline in approximately an East-West direction. The pads permit element separations of 120, 420, and 900 feet. The facility has little surrounding blockage and permits essentially hemispherical coverage by the array.

Preamplifiers

Solid state preamplifiers were used in the system and were mounted on the antennas for best system noise figure performance. The preamplifiers provided a nominal gain of 30 dB with a 3 dB bandwidth of 10 MHz. The pre-amps used in

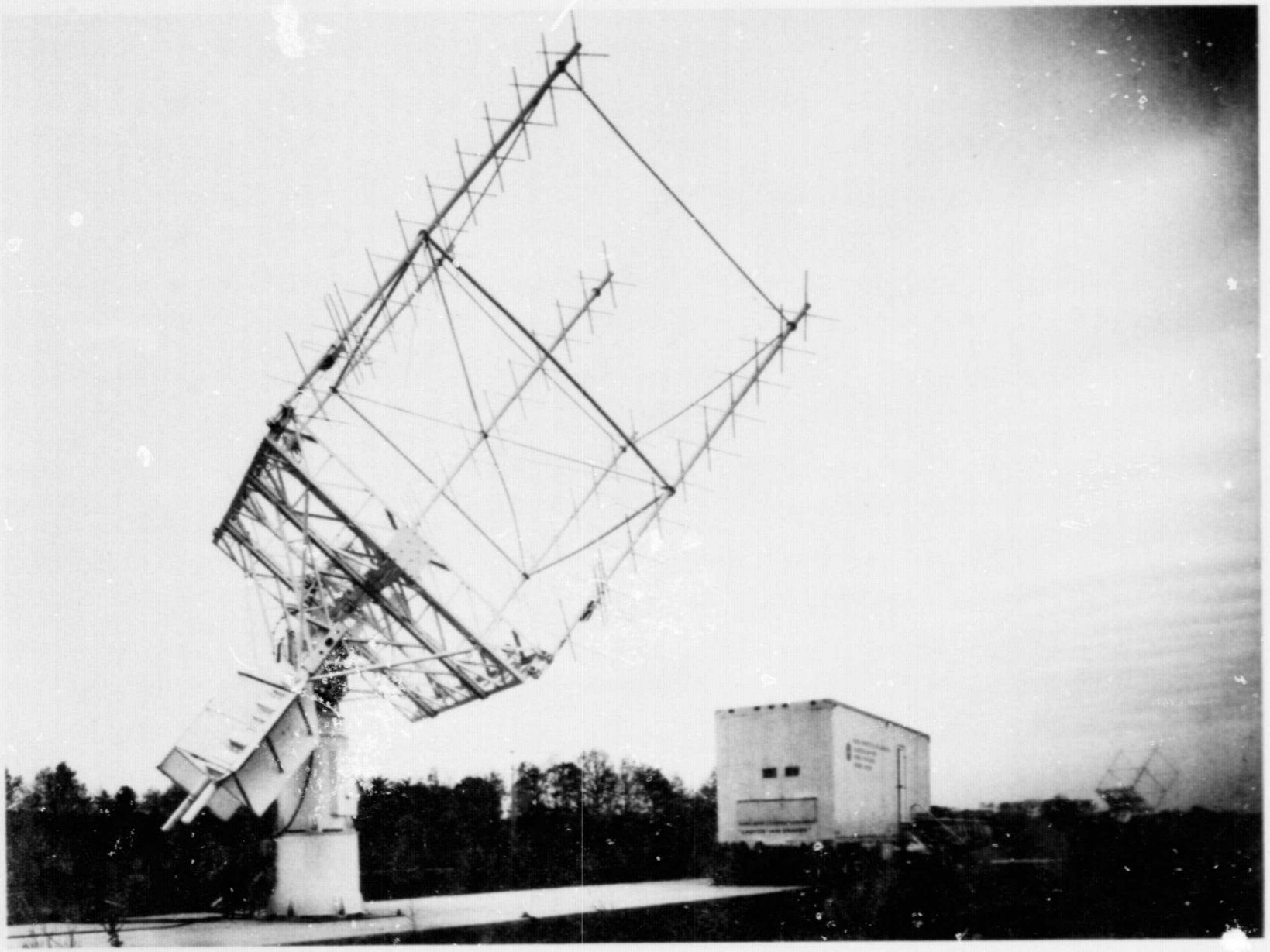

Figure 1. Two Element VHF Array and Electronics Van

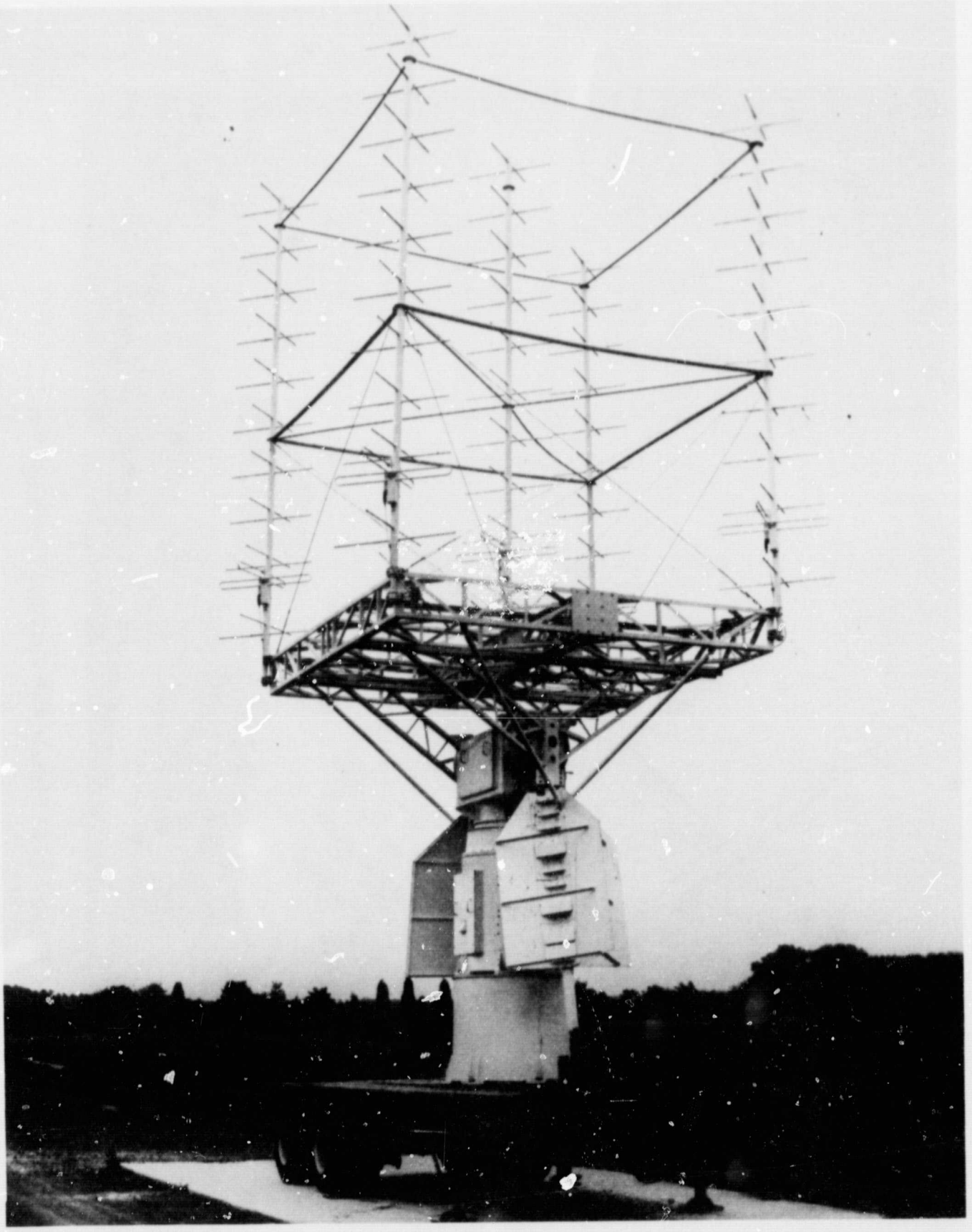

Figure 2. Movable Yagi Antenna

the sum channels of the antennas were chosen to match their noise figures at 3.5 dB. Semi-rigid coaxial cables were used between the antennas and electronics van (Figure 1). The cable length varied with antenna separation but was identical for each antenna at any given spacing.

Receiver

A signal transmitted from a spacecraft will in general differ in phase and frequency when received at the array elements. The received carrier will contain a doppler frequency shift determined by the relative velocity of the spacecraft with respect to the receiving antenna. The doppler shift is given by

$$F_d = \frac{v_r}{c} F_0 \qquad (1)$$

where:

F_d = doppler frequency shift

v_r = relative velocity

F_0 = carrier frequency

c = velocity of light

The relative velocity of spacecraft to ground station will in general be unique, and the v_r seen by one antenna in an array will not necessarily be equal to that for any other array element. Figure 3 shows the situation for a two-element array at a separation D. The relative velocity of the spacecraft seen by antenna 2 is then given by

$$v_2 = v_1 \cos \alpha$$

where

$$\alpha = \sin^{-1} \left(\frac{D}{R_1} \sin \beta \right)$$

and from Equation 1 we have

$$F \text{ differential} = F_1 - F_2 = \frac{v_1}{c} F_0 \left\{ 1 - \cos \left[\sin^{-1} \left(\frac{D}{R_1} \sin \beta \right) \right] \right\} \qquad (2)$$

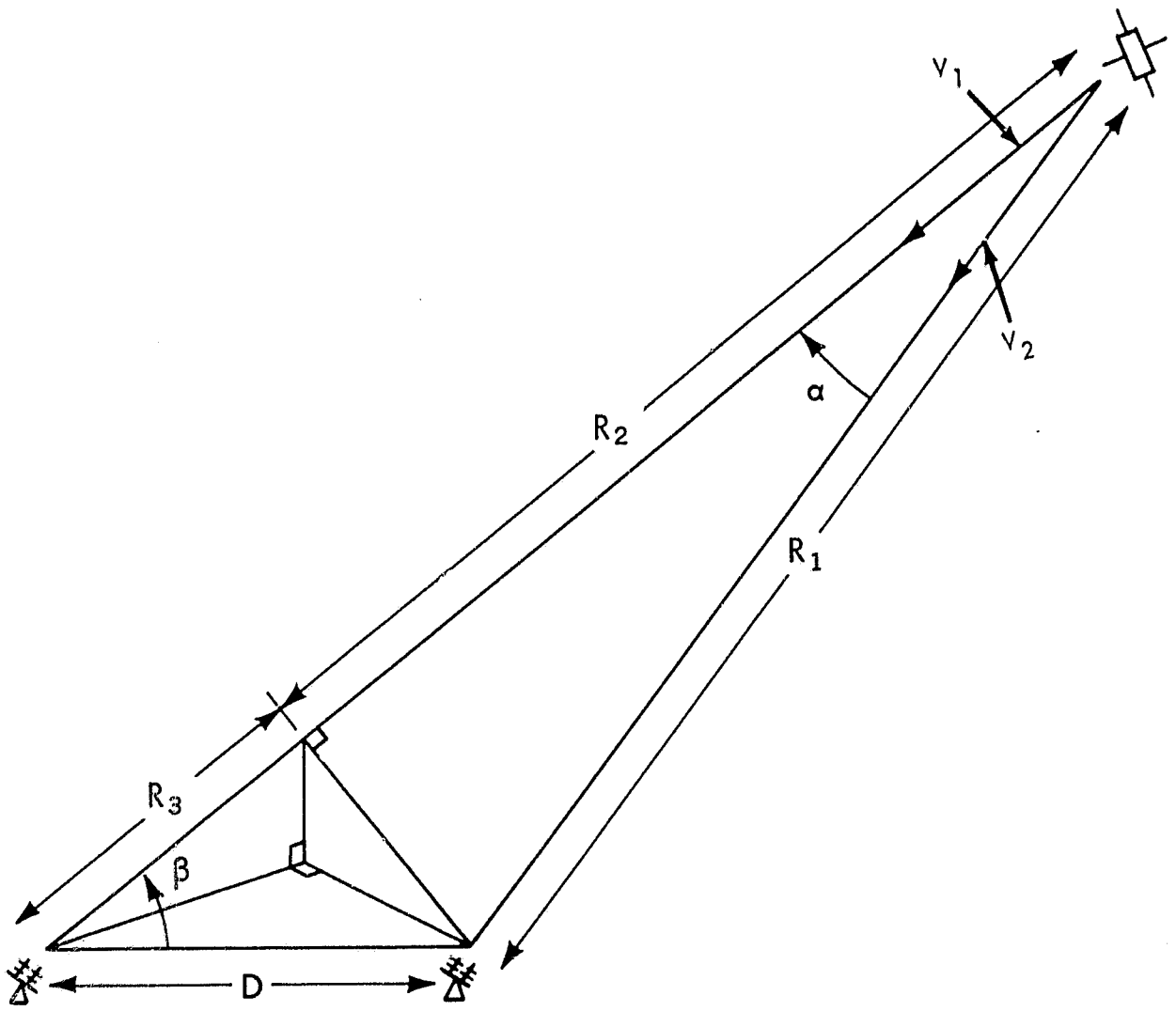

Figure 3. Geometry for Calculation of Differential Doppler Frequency Shifts

From Equation 2 we note that the differential doppler frequency shift is a function of the transmitted frequency as well as the orbital and array characteristics. At the VHF frequencies considered in the present antenna combining project, the differential doppler at a 900 foot spacing did not exceed one hertz for the spacecraft used.

The receiver used for this system was therefore required to coherently combine signals which in general are of different phase and frequency. The process is complicated by the doppler frequency shifts common to both antennas which can vary ±3 kHz, typically, about the transmitted carrier. These requirements are similar to those encountered in polarization diversity situations. The APDAR receiver, developed to meet the needs of polarization diversity,[1] was found to satisfy all the requirements anticipated for antenna combining. In addition, the APDAR provided an economical way of experimentally investigating the practical limitations and capabilities of antenna combining without a significant outlay for development of an entirely new receiver.

The APDAR receiver uses three phase lock loops (PLL) to perform the coherence operation (Figure 4). Each input channel is heterodyned to 11 MHz and locked to an internally generated reference. The 11 MHz signals are then combined and the output is supplied to a third PLL that closes on each of the input channels. The input PLL's are second order and provide good phase control[2] up to ±5 kHz from the carrier. The combined loop is third order and provides the ±250 kHz operating range required for large doppler frequency shifts. The receiver was designed to operate at frequencies up to 10 GHz and therefore provides more operational range than required for the present VHF program already described.

The coherence conditions described above will be sufficient to realize maximum gain improvement when the received SNRs are equal in each channel. In general, however, the SNR will not be identical in all array elements and a weighting process must be included for optimum performance. The incoming signals must be weighted, as described by Brennan,[3] on the basis of SNR for the array to realize maximum improvement. The APDAR receiver performs weighted combining on an AGC (automatic gain control) basis,[4] a good approximation to SNR weighting if the noise levels in the receiver channels are approximately equal. The combined output SNR under these conditions will be the sum of the input power SNRs. The maximum theoretical improvement for a two-element array is given in Figure 5.

---

[1]Reference 4
[2]Reference 5, p. 23
[3]Reference 2
[4]Reference 4, p. 673

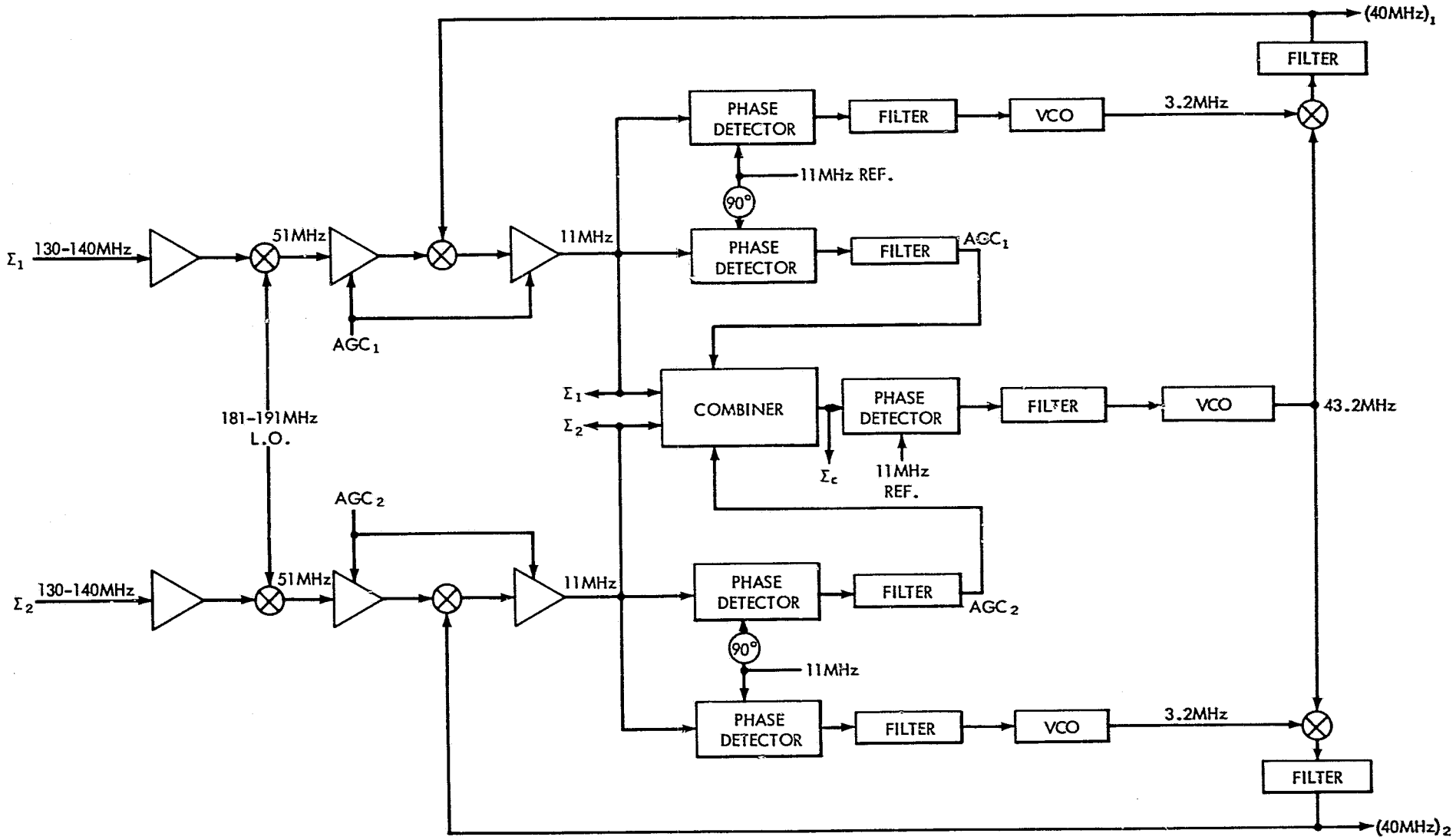

Figure 4. Block Diagram of Coherent Combiner

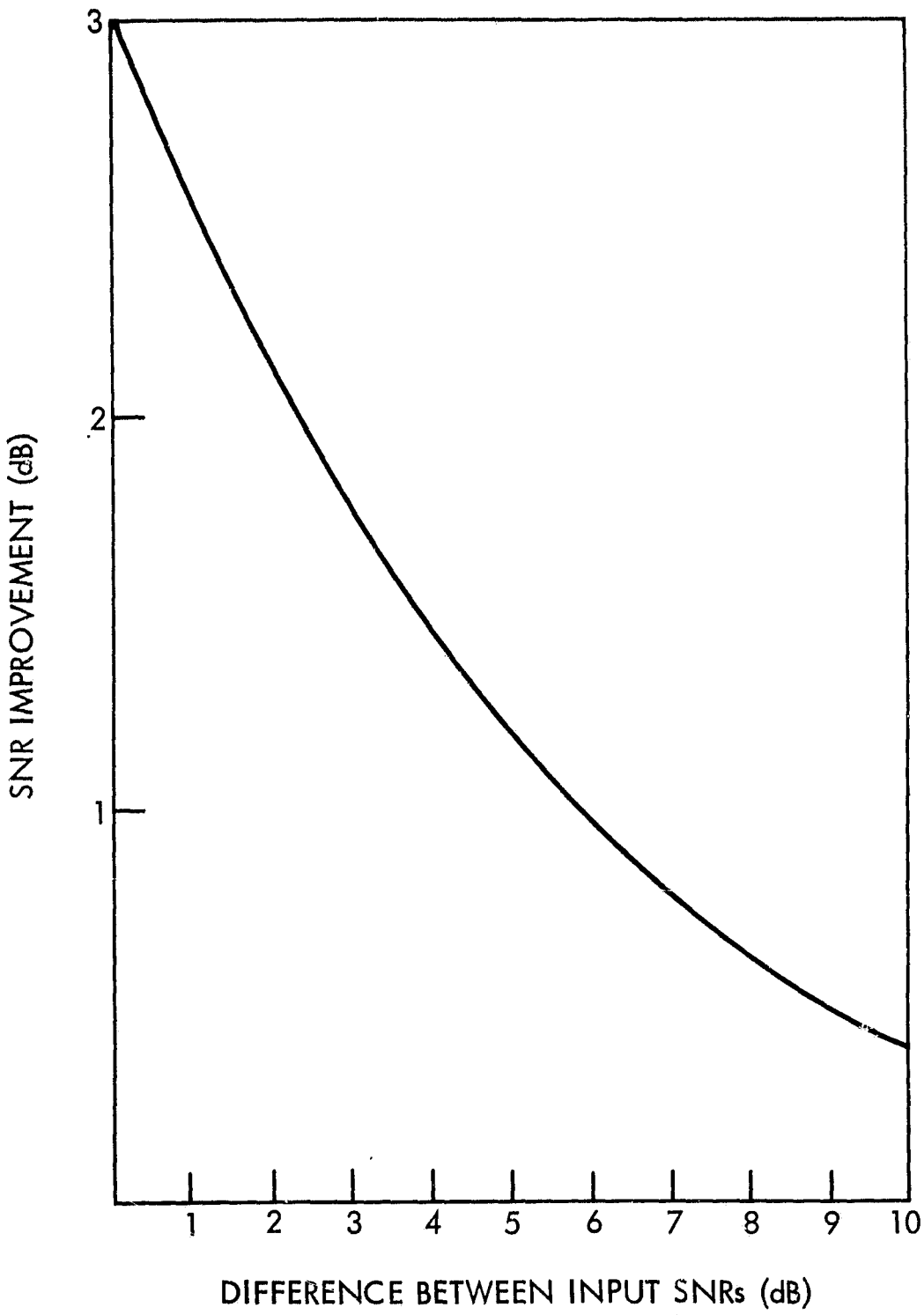

Figure 5. Maximum Theoretical SNR Improvement Versus Input Conditions

Time Delay System

The receiver characteristics already described are sufficient for an array of closely spaced elements. The coherence operation is based upon one cycle of the carrier and therefore is incapable of correcting for time delays in reception between the array elements. The physical situation is described in Figure 6 where the required delay correction is a function of satellite position and antenna separation. The delay correction is unnecessary for CW reception. When modulation is present, however, the transmission path differences can degrade the information output SNR after combining. The degradation will be a function of delay and modulation frequencies and can be significant in a future operational network. A time delay correction system was therefore included in the antenna combining project to determine it's effects on system operation.

The time delay units were inserted in the receiver IF stage as in Figure 7. The master antenna contained a fixed delay of 2.909 microseconds. The delay in the slave antenna was digitally variable from zero to 5.727 microseconds in 90.9 nanosecond-increments. The delay system block diagram is given in Figure 8. The delay increments were achieved with coils of RG 178B/U coaxial cable. Amplifier stages in each delay increment were adjusted to maintain a gain of zero for any delay setting. The system is capable of meeting the delay correction requirements[1] of an array with antenna separations of up to 2860 feet.

The time delay system was built by Philco-Ford Corporation to meet the antenna combining requirements. Tests have indicated that the delay system can maintain less than five degrees of phase error over the entire operational range, with a maximum gain of ±0.5 dB. A manual delay control switch was used for initial evaluation, but a fully operational system would contain automatic switching controlled by azimuth and elevation encoder position information from the tracking antennas.

EXPERIMENTAL PROGRAM

The investigation considered in this report has been primarily concentrated on two areas. The first of these concerns the SNR[2] improvement that can be practically achieved with the APDAR receiver. Test reports on this receiver[3] have not described the receiver under operational conditions in sufficient detail to warrant a firm decision as to its usefulness in antenna combining. A program

[1] Appendix A

[2] SNR (signal to noise ratio) shall be equated with carrier to noise ratio for those cases where there exists modulation on the carrier signal. This convention shall be maintained throughout the report.

[3] Reference 6

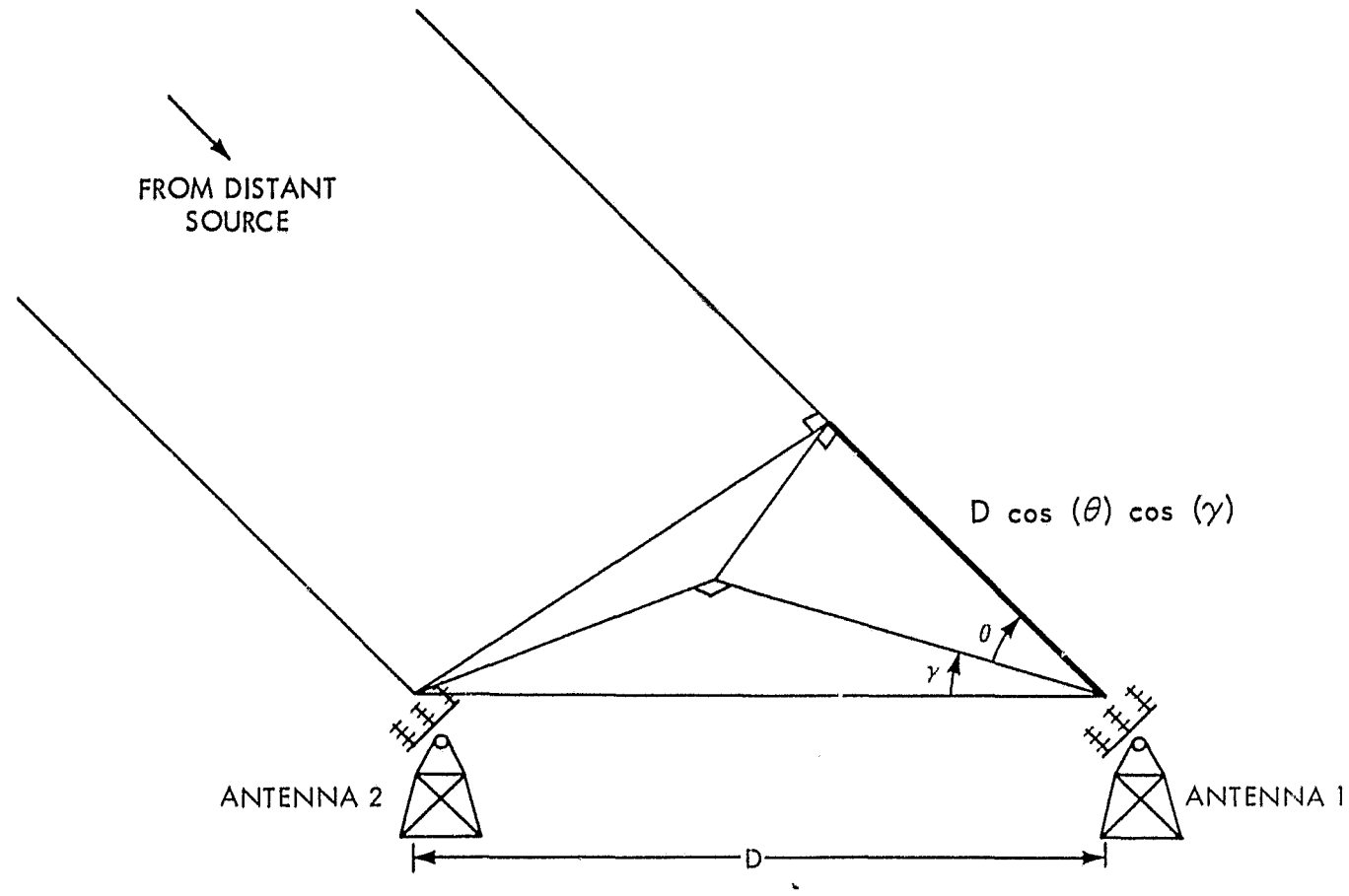

$T = \frac{D}{C}$ COS (θ) COS (γ) SECONDS

γ = AZIMUTH ANGLE OF SOURCE REFERRED TO BASELINE
θ = ELEVATION ANGLE OF SOURCE
C = VELOCITY OF LIGHT
D = ANTENNA SEPARATION

Figure 6. Geometry of Time of Arrival Delay

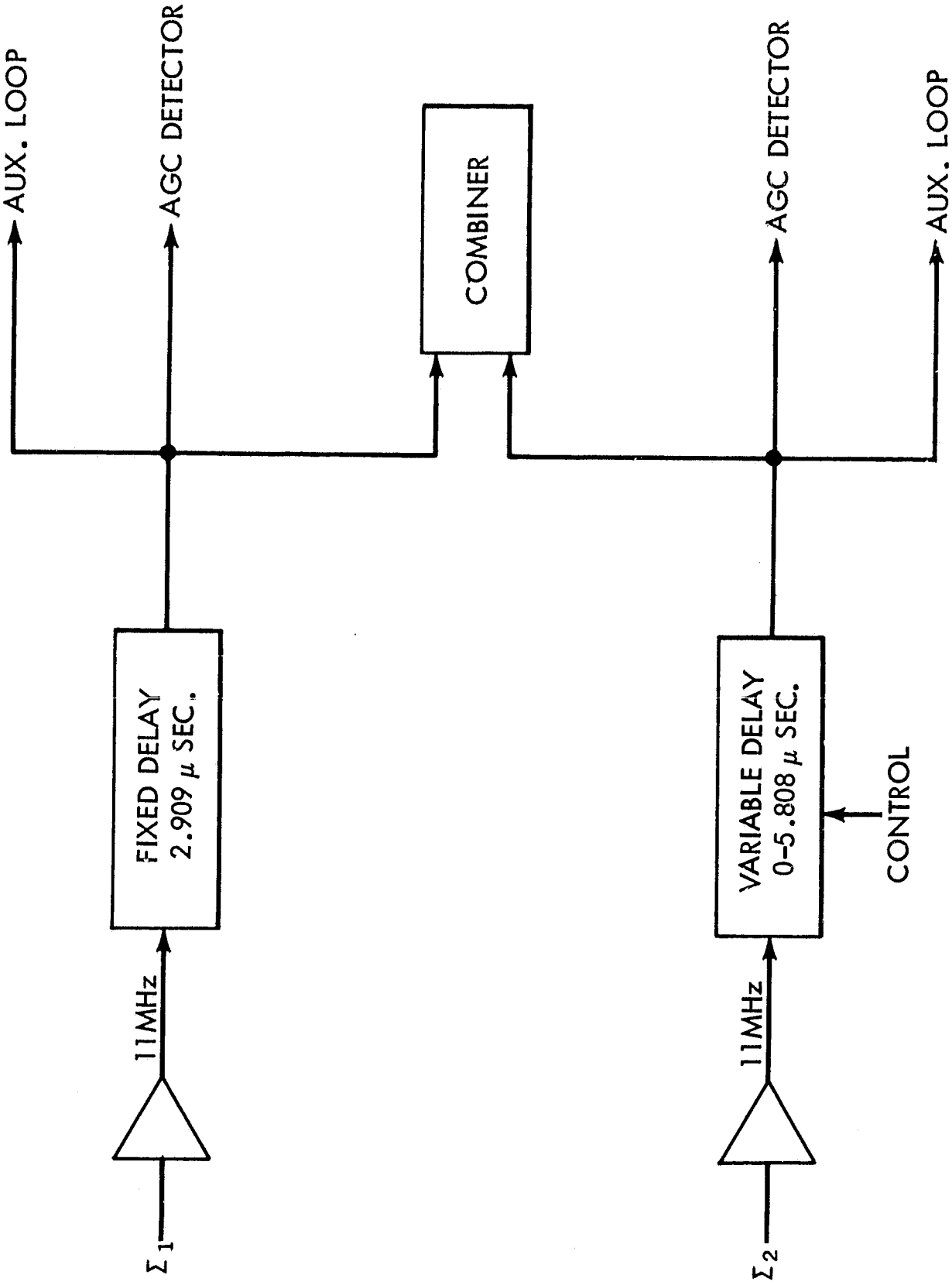

Figure 7. Incorporation of Time Delay System Into the Receiver

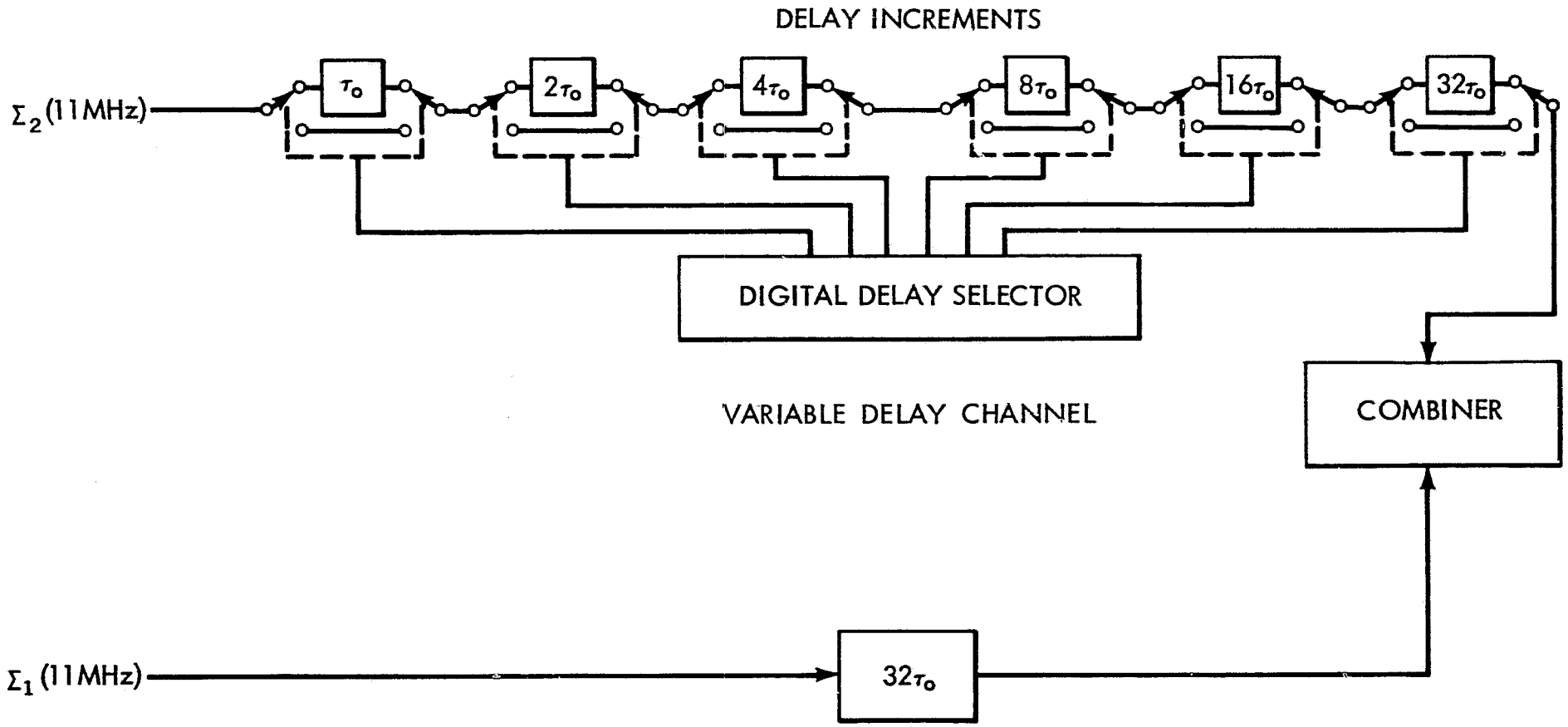

Figure 8. Block Diagram of Time Delay Compensation System

was necessary to determine the effectiveness of the APDAR as the combiner and to list the practical requiremonts of an adaptively phased large aperture array.

The second area of interest concerned the relative phase of the signals received at the array elements. Phase front distortion of the transmitted signal from atmospheric inhomogeneities will cause phase variations at the array elements.[1] These are in addition to that caused by differential doppler shifts and time delay. Relative phase measurements will define the requirements of the individual input channels of the receiver and would aid in describing phase front distortion. Figure 9 gives a block diagram of the scheme developed for measuring SNR improvement and relative phase.

Signal-to-Noise Ratio

The gain improvement realized from antenna combining is determined by measuring the SNR of the combined output and comparing it to that of the best input channel. Combining is performed at 11 MHz in the APDAR receiver (Figure 4). A coherent automatic gain control maintains the signal (S) level at IF essentially constant over its operating range. The 11 MHz level measured, however, contains signal plus noise (S + N) and can vary from -35 dBm to -5 dBm, typically. The problem, therefore, was to measure the SNR when the S + N can cover a 30 dB range.

The experiments involved simultaneously measuring the S and S + N levels. The SNR could then be calculated from the relation

$$SNR = \left[\frac{S}{(S+N)-S}\right]_{dB} + N.F. \qquad (3)$$

where N.F. refers to the noise figure of the detection circuitry. As shown in Figure 9, S was measured with a coherent detector. An RMS voltmeter simultaneously measured the S + N and both quantities were recorded. The noise figure of the detection circuitry was a known constant and the SNR was calculated.

Practically, the SNR calculation would not be continuous but would be determined at discrete intervals. The discrete nature of the output made possible the use of a single detection circuit for the three IF channels: Σ_c, Σ_1 and Σ_2. The process involved using an electrically controlled coaxial switch. The switch was actually composed of three 3-port coaxial switches as in Figure 10. By appropriately setting each switch, any one of four output ports could be sampled. The sampled channel is amplified and heterodyned to the 3.25 MHz input frequency of the coherent detector. The S and S + N levels then permit a calculation of SNR as described previously.

[1] Reference 1, pp. 35-40

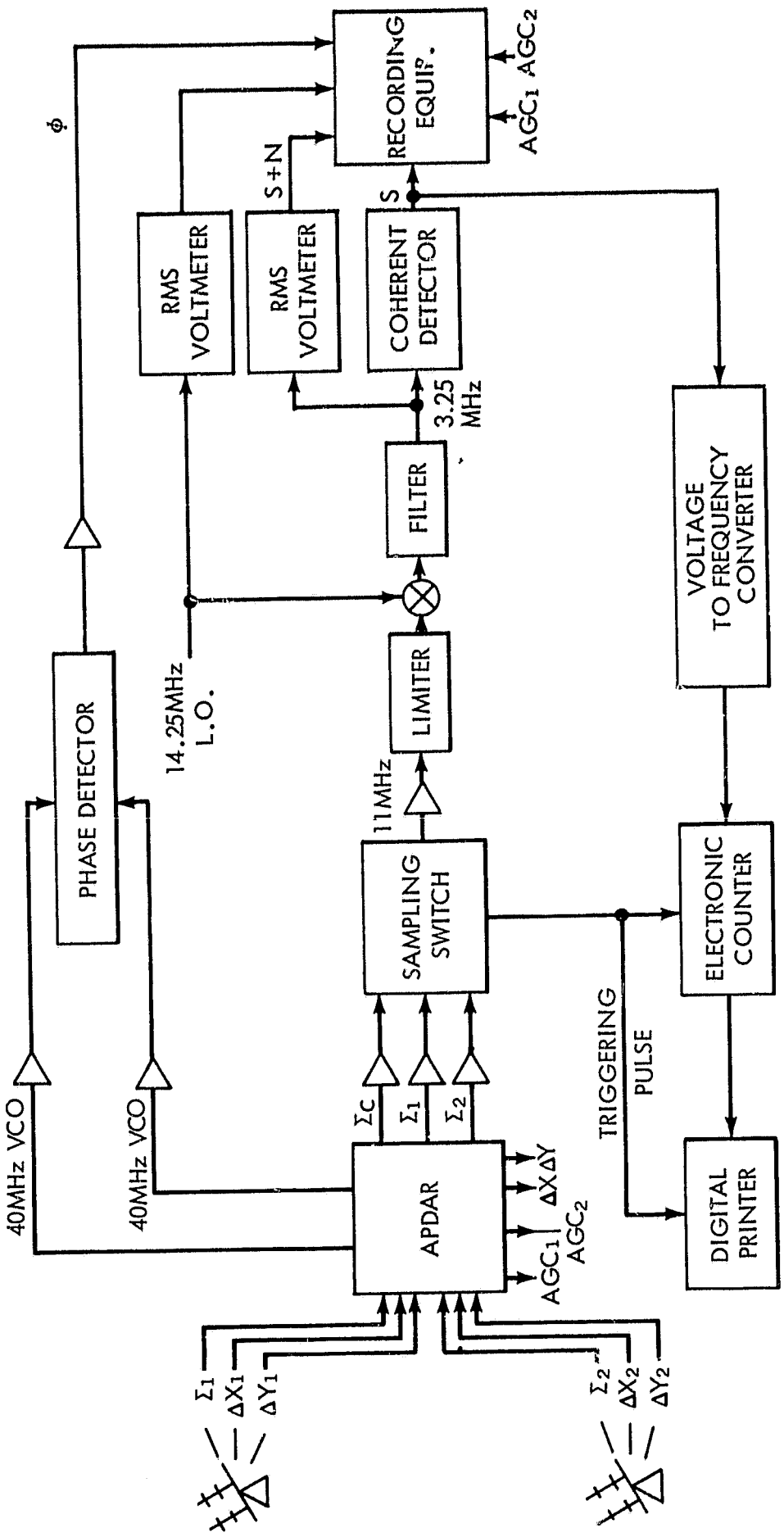

Figure 9. Block Diagram of Measurement Scheme

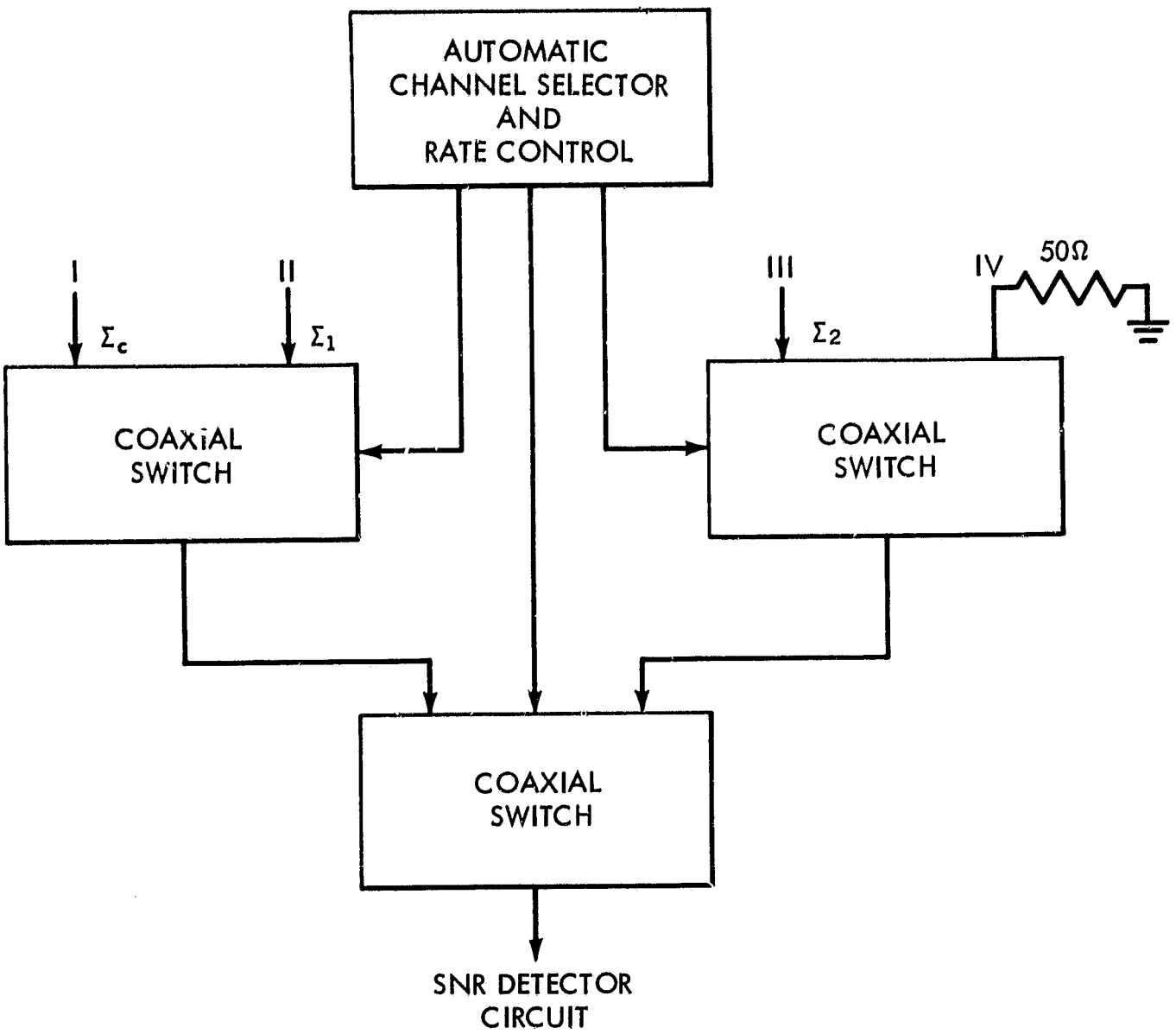

Figure 10. Sampling Switch

In order to reduce the amount of required data and to facilitate calculations, the S + N level was maintained constant with a hard limiter prior to mixing. The addition of the limiter complicates the calculation of SNR and an added relation[1] must be satisfied:

$$SNR_0 = (SNR)_i \frac{1 + 2(SNR)_i}{4/\pi + (SNR)_i} \qquad (4)$$

where:

SNR_0 = S/(S + N) - S of Equation 3

SNR_i = SNR at the output of the IF amplifiers prior to limiting

Equation 4 must therefore be solved for SNR_i, which then replaces $[S/(S + N) - S]$ in Equation 3.

The sampling operation described above was performed automatically at a fixed rate. The switching rate determines the sampling period for any one channel and can be continuously adjusted up to five seconds. The rate is limited by the coherent detector stabilization time and the recording instruments used. Figure 11 gives an example of the coherent detector output as a function of time for a sampling period of five seconds. The synchronization pulse in the strip chart represents no sampling input signal, designated by input port IV of Figure 10. The sampling pulse allows an observer to easily identify each of the Σ_c, Σ_1, and Σ_2 channels on any recording.

The sampling switch causes a mismatch in the sum channels of the receiver and creates transients in the entire system. This problem was eliminated by inserting a 10 dB 11 MHz amplifier and emitter follower in each sum channel between the receiver and switch. The amplifiers were constructed identically and the noise figure from the amplifier input to the mixer output was 14 ± .1 dB for each channel.

The strip chart recording of Figure 11 indicates the noise present on the coherent detector output. Accurate measurements of S required the elimination of the noise component. The AGC output was voltage to frequency converted and averaged over two seconds with an electronic counter. The counter must be triggered by the sampling switch to insure synchronization. The electronic

[1] Appendix B

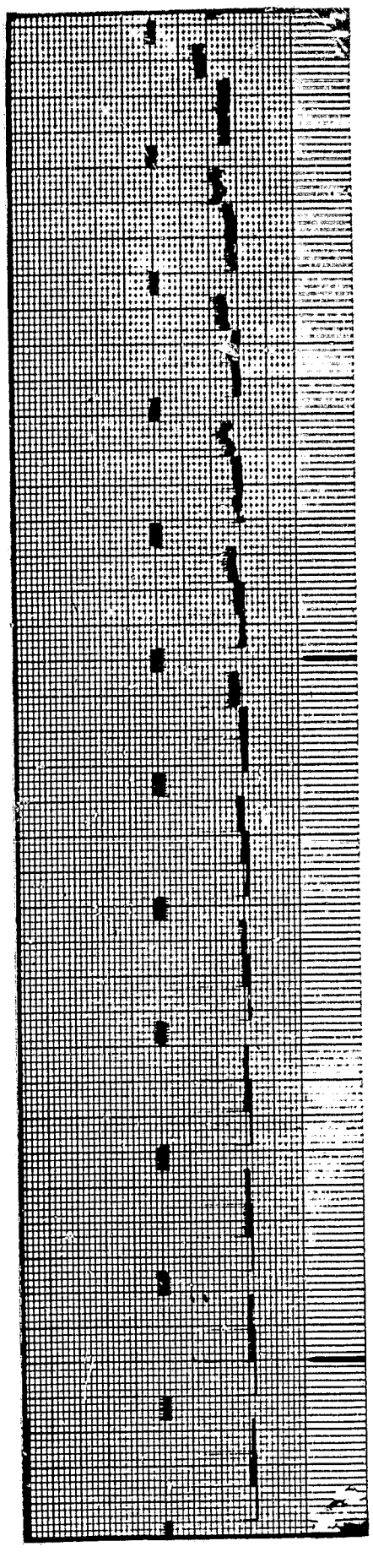

Figure 11. Strip Chart Recording of Coherent Detector Output for RELAY II Under Severe Fading Conditions

counter could then interface with a digital printer to provide the averaged output (Figure 9). The system was adjusted to allow two seconds for the coherent detector to lock and stabilize, two seconds for averaging, and one second to switch and reset the counter.

Phase

Detection of the relative phase between signals received at the two antennas was a much simpler process than that required for SNR measurements. The SNR at the 11 MHz IF varied, typically, from 16 dB for RELAY II to 0 dB for ATS-C. The relative phase measurements should be as independent of the received signal levels as possible to reduce the noise contributions in low SNR situations. The APDAR receiver described earlier (Figure 4) provides independent automatic gain control to each input channel. This AGC process minimizes the effect of incoming signal level variations, permitting the phase detectors used to control the PLLs to operate on a constant 11 MHz input. The phase detector output then modulates a nominal 3.2 MHz carrier for each input channel. A similar process is performed in the combined sum channel with the phase information modulating a 43.2 MHz carrier. The order of the filters used in the input and combined channels are such that the doppler frequency shifts are supported by the 43.2 MHz and the lower frequency phase changes by the 3.2 MHz carrier.

The 43.2 MHz VCO output is mixed with each 3.2 MHz signal and the corresponding 40 MHz components are used in the second mixing stage of the receiver. Each 40 MHz signal then contains the following components:

$$S_1\,(40\,\text{MHz}) = A_1 \cos\left[2\pi\left(F_0 + Fd_1\right)\,t + \theta_1\right]$$

$$S_2\,(40\,\text{MHz}) = A_2 \cos\left[2\pi\left(F_0 + Fd_2\right)\,t + \theta_2\right]$$

where:

F_0 = 40 MHz nominal

Fd_1, Fd_2 = doppler frequency shifts seen at each antenna

θ_1, θ_2 = phase difference between each input channel and the receiver reference.

The magnitude of A_1 and A_2 are determined by the VCO output levels and are essentially constant. By mixing the two 40 MHz signals together, followed by a

low pass filter, the output will be:

$$\phi = \frac{A_1 A_2}{2} \cos \left[2\pi \left(Fd_1 - Fd_2\right) + \left(\theta_1 - \theta_2\right)\right] \tag{5}$$

where $Fd_1 - Fd_2$ represents the differential doppler frequency and the higher frequency phase variations caused by the propagation medium. The $(\theta_1 - \theta_2)$ term contains the relative phase due to path length differences and to constant phase differences in the two channels. The ϕ given by Equation 5 is the relative phase difference between the received signals and was recorded on magnetic tape for later processing.

This technique offers several desirable features in performing the relative phase measurements. The more significant of these features are given below:

1. Completely eliminates the overall doppler frequency components.
2. Provides measurement accuracy equal to that performed in the APDAR receiver.
3. Minimizes the effect of incoming signal levels.

Data processing of the magnetic tape recordings then provides a spectrum of the frequency components in the experimental data and their respective magnitudes.

RESULTS

The experimental program, including the measuring techniques employed, have already been described in detail. The results from the experiments must be studied in light of the procedure used to arrive at the data. The SNR test results and the relative phase test results will be given separately along with an interpretation of their meaning. The discussion of the signal-to-noise ratio improvement during satellite experiments will be preceded by the results of calibration tests performed to establish the capability of the combiner.

Signal-to-Noise Ratio

Evaluation of the APDAR receiver as a combiner was performed by inserting independent SNRs into each input channel and measuring the improvement with the detection equipment described in the Experimental Program section of this report. The calculations required to arrive at the SNR from the measured S and

S + N data were performed by a computer program in all cases. The calibration tests were run to determine the maximum improvement possible for any given input SNR within its operating range and to determine the improvement when the input SNRs are unequal. The maximum theoretical output SNR will be related to that of the best input channel as in Figure 5.

The curve of Figure 12 represents the measured improvement with identical input SNRs in each channel. The dashed line gives the 2.5 dB minimum performance specification for the receiver and indicates good agreement with the measured data. The curve shows that the calibration tests give a minimum of 2.45 dB improvement as compared to a 3.0 dB maximum theoretical value throughout the operational range of the detection circuitry.

The effects of changing the relative input SNR levels are given in Figure 13. The two solid lines represent results for constant SNR_1 levels of -0.6 dB and +4.5 dB. The abscissa of the graph represents the relative input SNR levels achieved by varying SNR_2 only. The dashed line shows the maximum theoretical improvement and the broken line gives the minimum performance specification for the receiver. The values of SNR_1 used for this illustration were chosen to cover the range of conditions typical for ATS-C experiments which will be described later. These SNR_1 values place the tests near the worst operational range of the combiner (Figure 12) and are therefore a conservative estimate of the capability of the receiver.

The characteristic of the combiner to fall away from the minimum performance curve as the relative input SNR increases is a measure of a deficiency in the receiver weighting process. The APDAR receiver performs the weighting function on an AGC basis. The calibration tests were therefore arranged to provide equal signal and equal noise levels in each input channel. The relative input SNR was then changed by only varying the signal level in channel two. The tests were performed in this manner to adapt to the receiver weighting process[1] which estimates the SNR on the basis of signal level only.

The satellite experiments concentrated on the use of RELAY II, ESSA 6 and ATS-C as the transmitting sources. The 136.62 MHz beacon from RELAY II gave a SNR of better than 14 dB, typically, at 11 MHz with the 30 kHz APDAR I.F. bandwidth. Accurate measurements of SNR greater than 10 dB are difficult with the present detection equipment. The limiter used to maintain a constant S + N level requires a precise measurement of S to permit calculation of the SNR. When the signal-to-noise ratio exceeds 10 dB, the accuracy of the measurements begins to degrade and therefore no attempt was made to perform meaningful SNR improvement tests at these levels. Since RELAY II gave a SNR of 14 dB, independent noise sources were used to reduce the SNR in each channel prior to combining to a level adaptable to the detection equipment.

[1]Appendix C

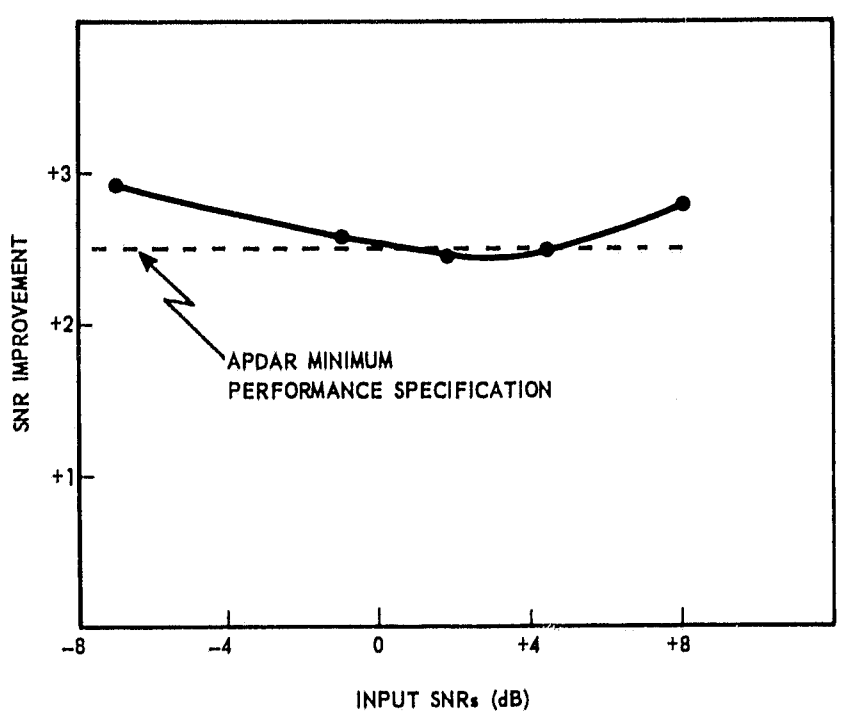

Figure 12. Combiner Performance Versus Input SNR (Identical in Both Channels)

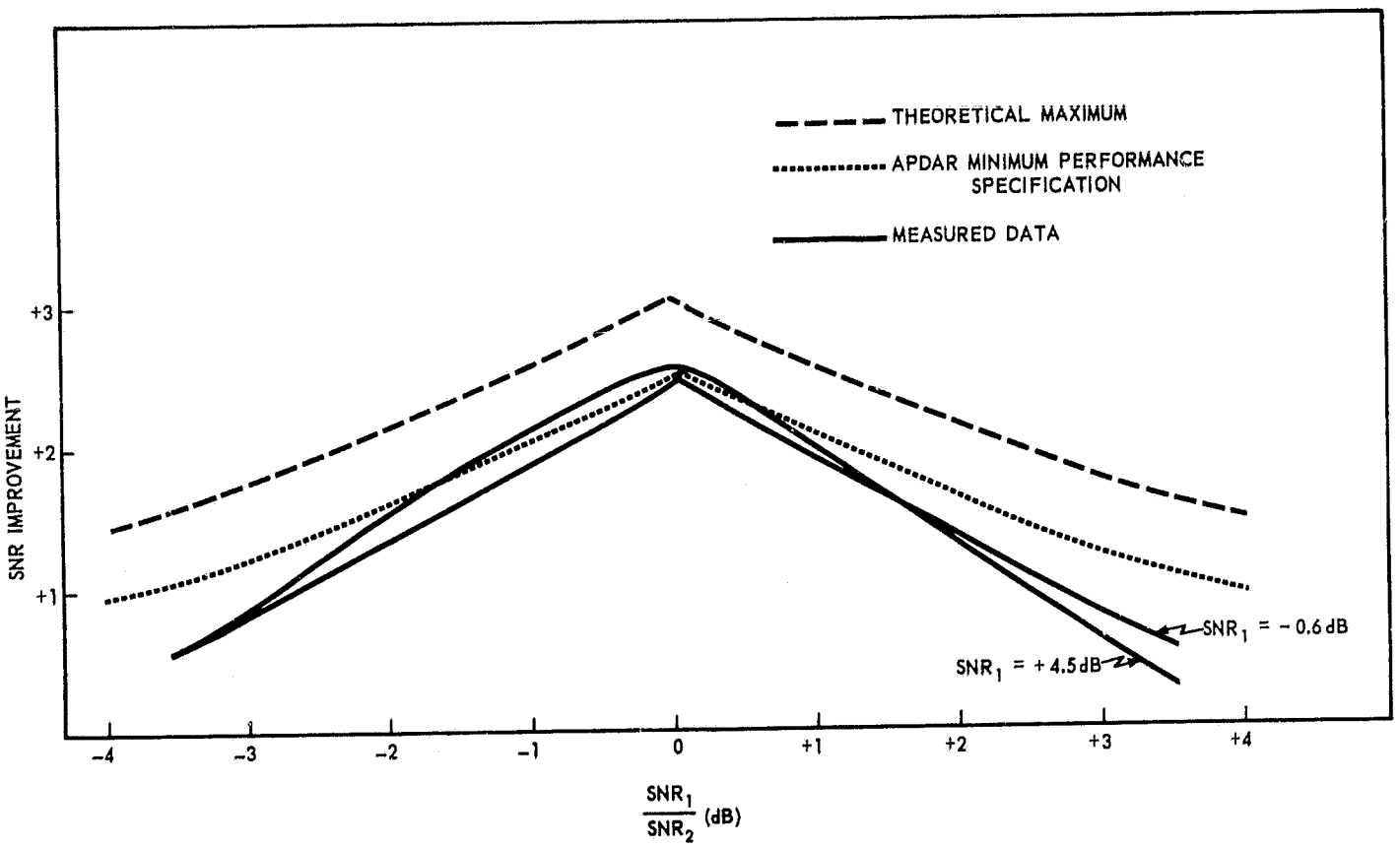

Figure 13. Combiner Performance Versus Difference in Input SNRs

The experimental results for RELAY II did not indicate any consistent improvement in SNR. This behavior was the result of two characteristics of the system that must be remembered to correctly evaluate the data. First, the capability of the detection system to give accurate SNR measurements requires that the SNR be essentially constant in all three channels for the time required for one sampling cycle. Figure 14 indicates a typical AGC record for RELAY II. The strip chart shows a constantly changing AGC level in each channel with few 15 second periods with the required constant AGC levels. This characteristic of RELAY II passes brings out the limitation in the measurement scheme and eliminates the use of RELAY II for evaluation of SNR improvement capability.

Secondly, the calibration experiments indicated that the combiner operates well only when the input SNRs are within a few decibels of being identical. Figure 14 indicates that the signal from RELAY II can differ by more than 5 dB between antennas and the SNR improvement seen at the output of the combiner will therefore be substantially reduced.

Experiments with ESSA-6 exhibited a variation in SNR less rapid than that seen with RELAY II, but when compounded with the periodic fluctuations due to satellite rotation (Figure 15) the result was again a situation unadaptable to the measurement scheme. The fading and fluctuations due to satellite rotation were more severe for channel two than for channel one in both RELAY II and ESSA-6 experiments. This phenomenon was reversed when the associated antenna outputs were switched at the receiver, and the characteristic is therefore not a product of the receiver but of the receiving elements. Attempts to remedy the situation at antenna two were unsuccessful.

The ATS-C experiments involved a range of SNR from -5.0 dB to +5.0 dB, typically, but unlike the other two satellites considered the ATS-C signals were maintained at constant levels for long periods of time. This characteristic made ATS-C an ideal source for the SNR improvement experiments. Figure 16 summarizes the results of six ATS experiments and shows the cumulative distribution of the measured SNR improvement. This curve represents the average results of 400 individual improvement calculations and therefore involved a total of 1200 separate SNR measurements.

Figure 16 shows only 36 percent of the data exceeding 2.0 dB improvement. It must be remembered that the measured SNR improvement is a function of the relative input levels as in Figure 13. The curve of Figure 16 although helpful in estimating the improvement capability of the present array is unable to show the distribution of expected SNR improvement based on the recorded input conditions. A better measure of the receiver capability can be achieved by plotting the distribution of the difference between the measured improvement and the theoretical

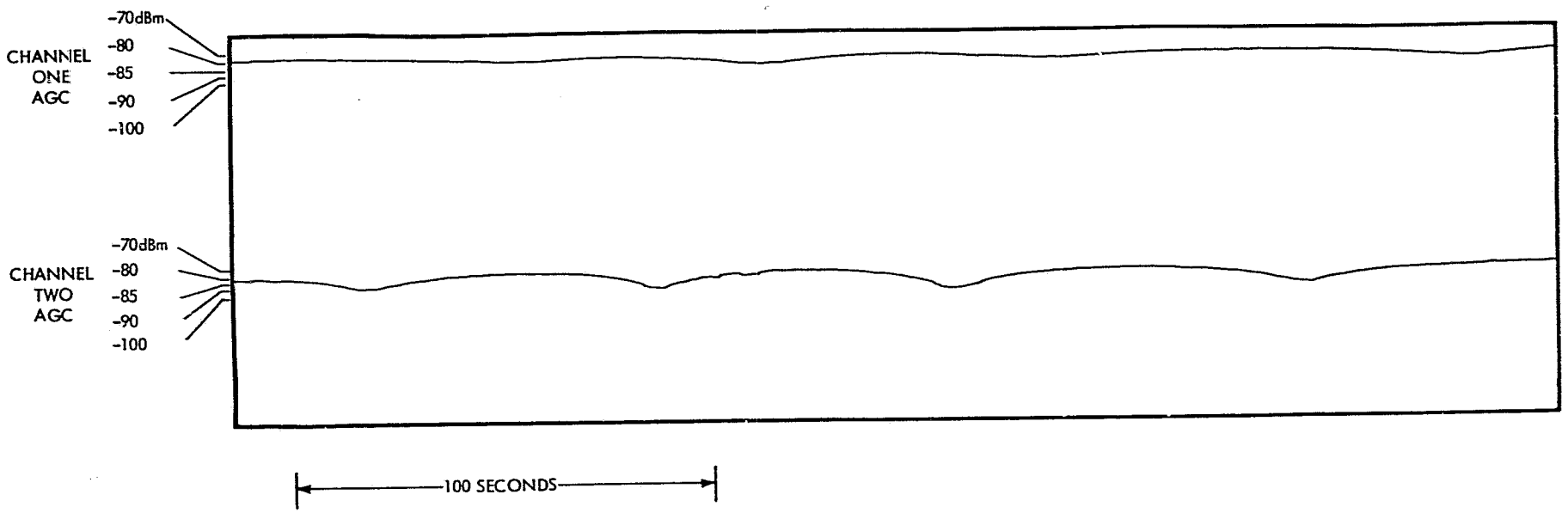

Figure 14. Typical RELAY II AGC Record, 180' Antenna Spacing

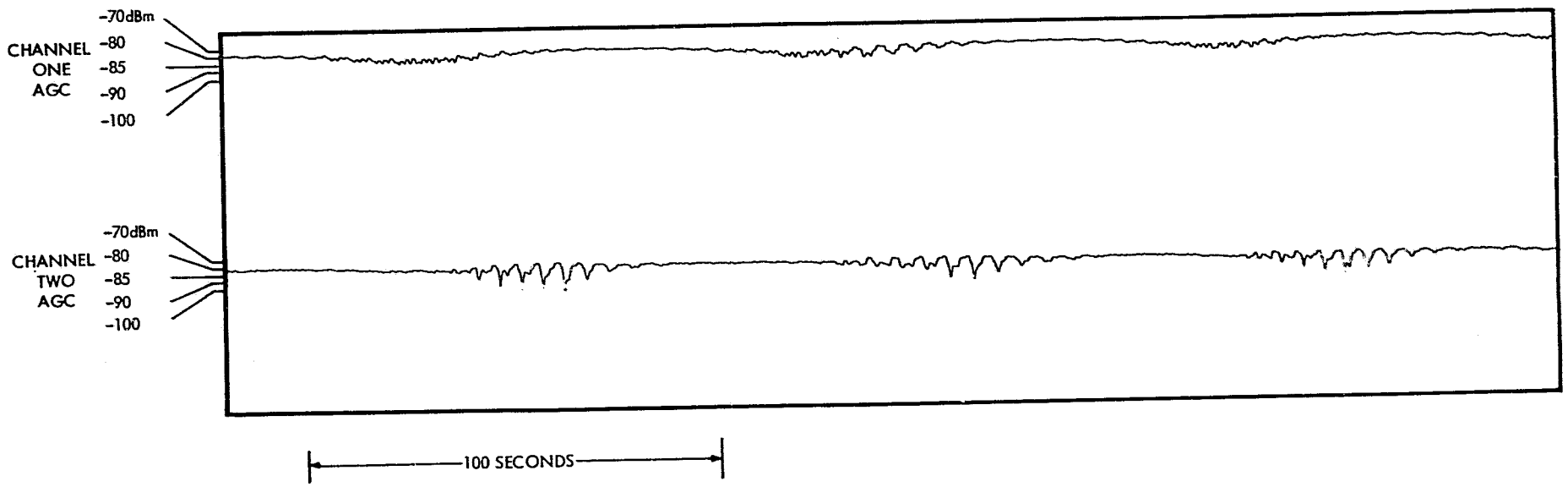

Figure 15. Typical ESSA-6 AGC Record, 440' Antenna Spacing

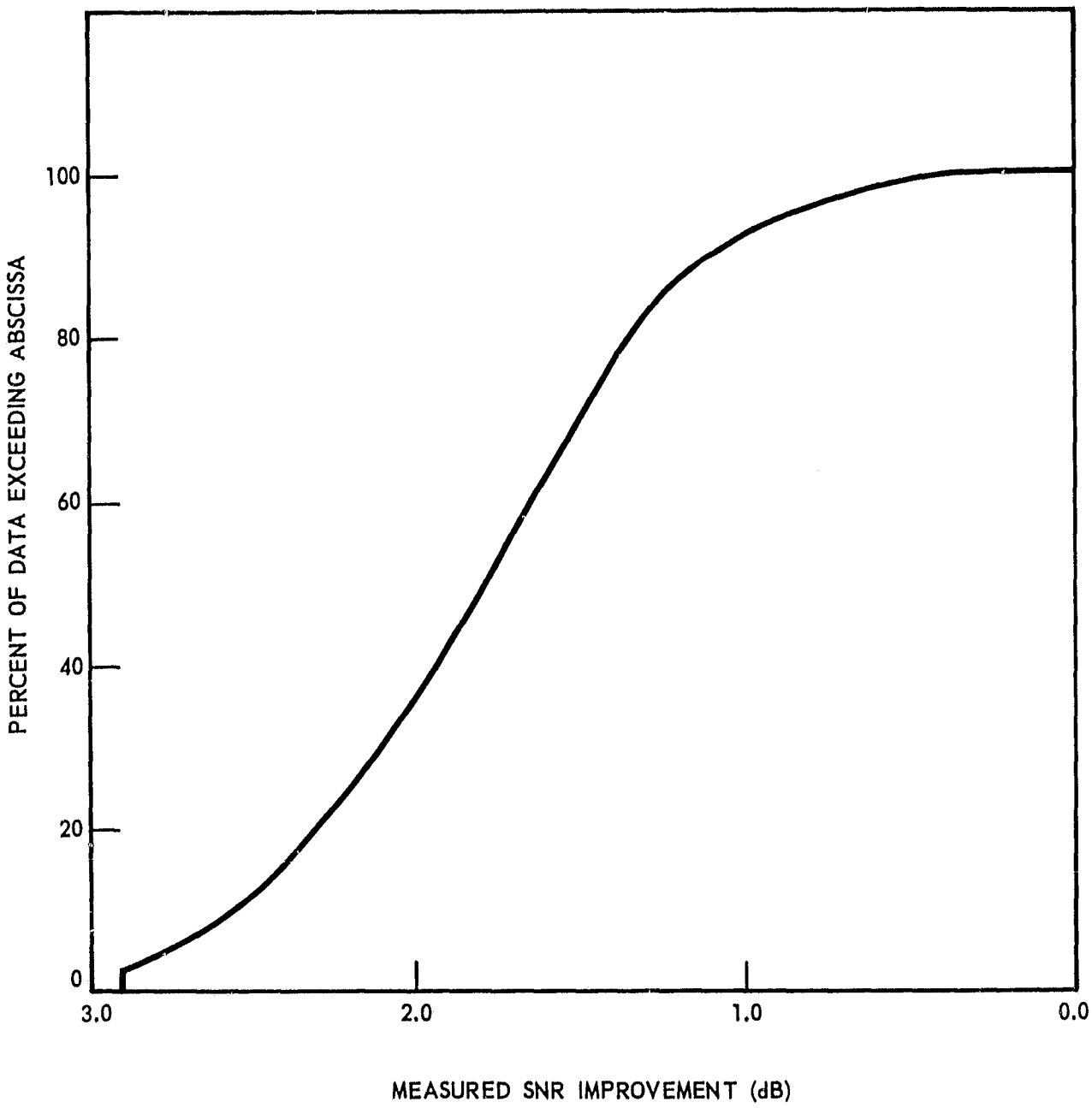

Figure 16. Cumulative Distribution of Measured SNR Improvement (ATS-C)

maximum as in Figure 17. In this form, the data can be seen to fall within the required minimum design goal (error $\leq$ 0.5 dB) 50 percent of the time.

The calibration tests (Figure 13) have already indicated that the weighting process performed in the APDAR receiver is not capable of holding the SNR improvement within the design goal. A third distribution was therefore made (Figure 18) to summarize the input conditions to the receiver during the ATS-C experiments. The ordinate here represents the percentage of the data for which the measured input SNRs differed by less than the corresponding value on the abscissa.

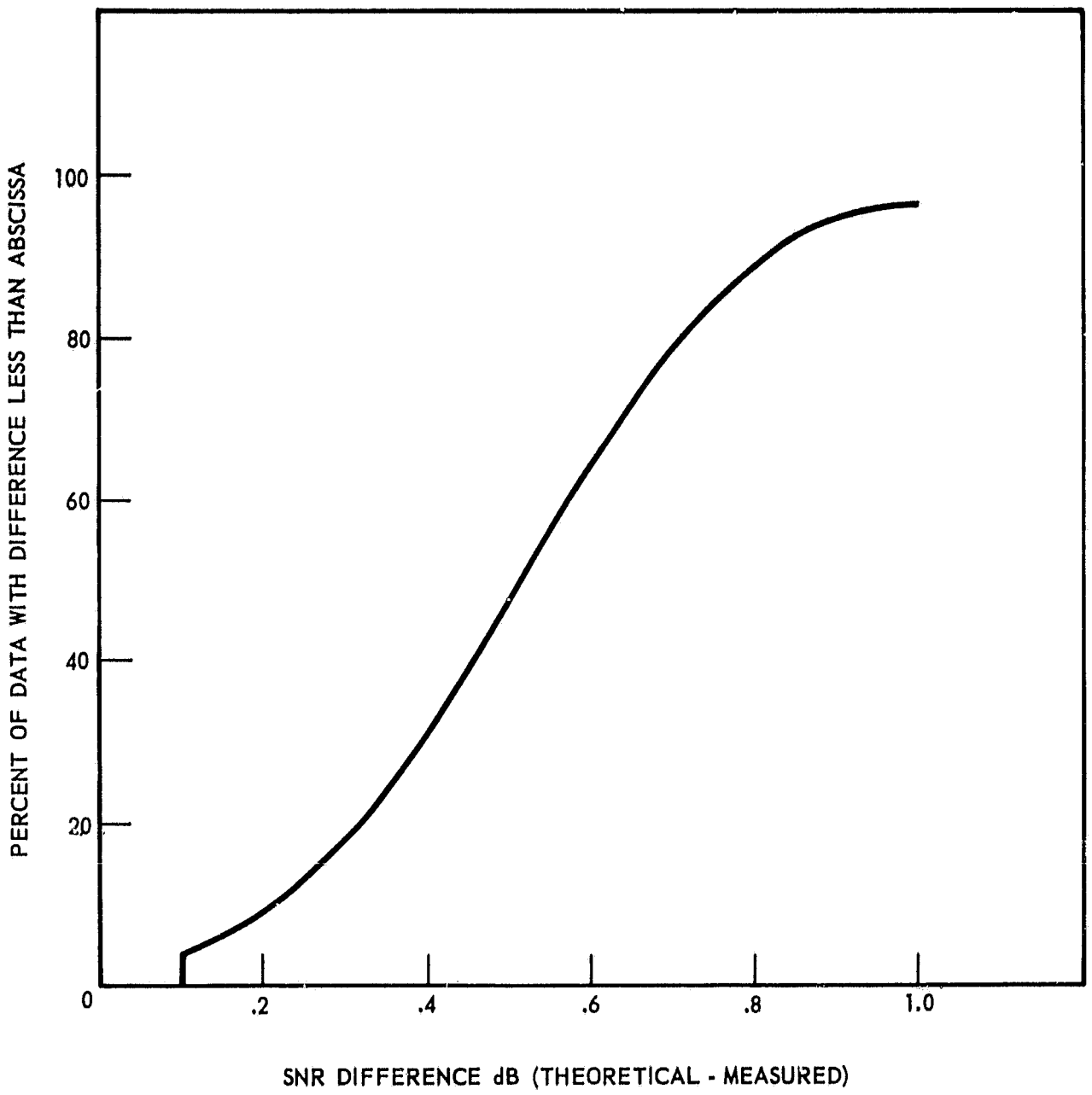

Figure 17. Cumulative Distribution of Difference Between Theoretical Maxima and Measured SNR Improvement (ATS-C)

Using the data in Figures 16 and 18 the performance of the APDAR receiver can now be evaluated based on the theoretical maximum of Figure 5. The most logical criterion for evaluation is the design goal of 0.5 dB difference between the experimental data and theoretical maxima. Table I gives the expected SNR improvement for four relative input tolerances. The third column lists the percentage of the measured data within the stated tolerance (Figure 18) and column four gives the percentage of the measured data achieving the minimum design goal (Figure 16). Table I therefore indicates that the combiner exceeded the 0.5 dB criterion for relative input SNRs of less than 3.0 dB. For input conditions exceeding this tolerance the receiver does not achieve the 0.5 dB criterion. This

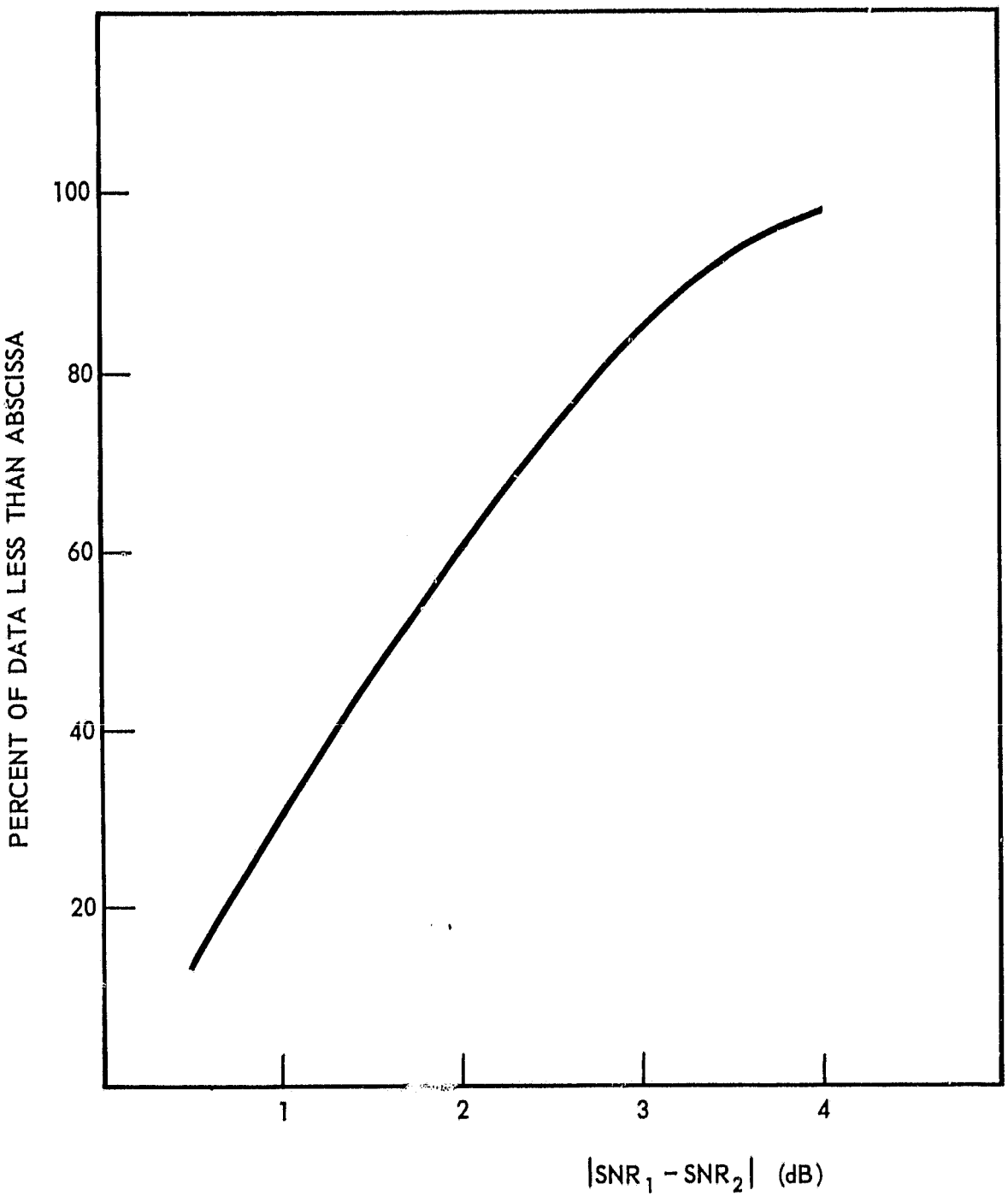

Figure 18. Cumulative Distribution of the Measured Relative SNR Levels Between Array Elements (ATS-C)

Table I

Summary of APDAR Performance

$\left(\frac{SNR_1}{SNR_2}\right)$ dB	Minimum Design Goal	Experimental Results	
	SNR Improvement	Percent Input Correlation	Percent SNR Improvement Correlation
±1.0 dB	2.0 dB	30%	36%
±2.0 dB	1.6 dB	60%	62%
±3.0 dB	1.2 dB	84%	87%
±4.0 dB	0.95 dB	97%	94%

analysis verifies the calibration tests of Figure 13 which indicated the inability of the weighting process to hold the SNR improvement to within the minimum design specification.

Phase

The relative phase between antennas was measured and recorded on magnetic tape. Spectral analysis of the data then permitted an evaluation of phase front characteristics and variations with time and antenna separation. An antenna separation of 180 feet resulted in a relatively calm response as shown in Figures 19 and 20. ESSA-6 showed significant response only for frequencies below 1 Hz, and these are predominantly due to changing time of arrival delay. RELAY II, however, contained repetitive frequency components of approximately 2.5, 4.5 and 6.8 Hz. These components were measured only with RELAY II and were present at all array spacings. These frequencies are felt to be characteristic of the satellite and related, in part, to its spin rate of approximately 2 rps as compared to 16 rpm for ESSA spacecraft.

The random phase components for the 180 foot spacing were relatively small for both satellites, but were increased substantially with increased antenna separation. Figures 21 and 22 give results at a 440 foot spacing. ESSA-3 indicates small random phase contributions over the entire frequency band investigated. RELAY II, however, contained relatively large random contributions at distinct frequencies, the frequencies being in general non-repetitive. The frequency components predominating at the 180' spacing were also present at 440'

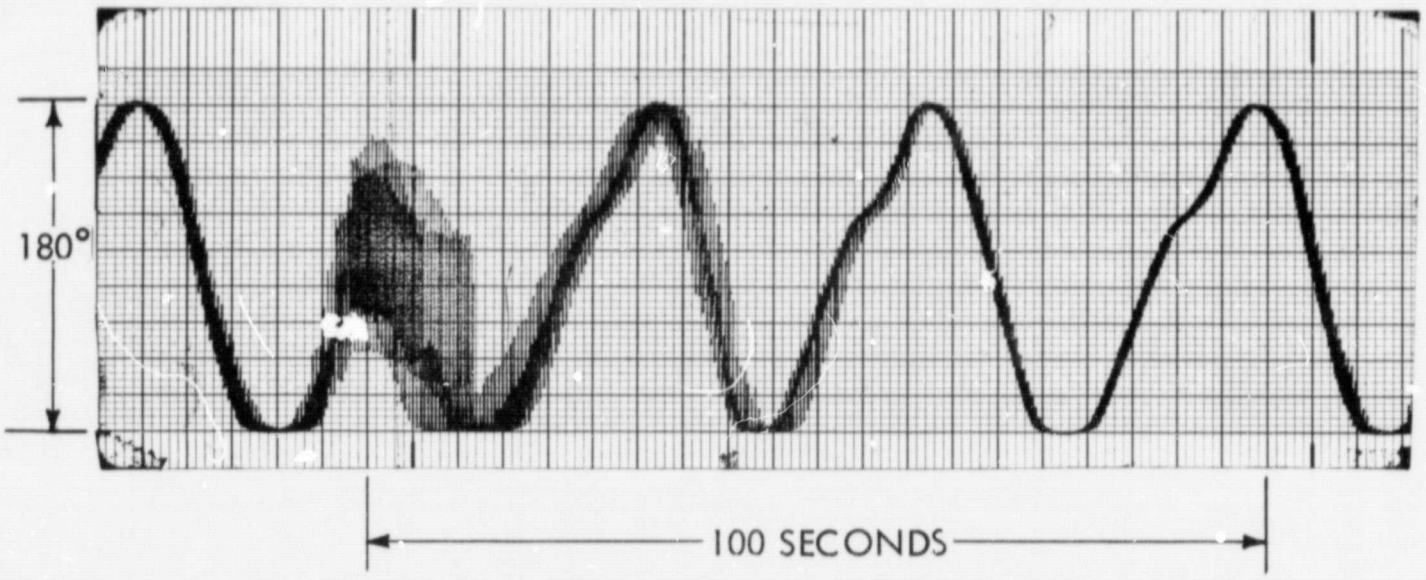

STRIP CHART RECORDING OF RELATIVE PHASE

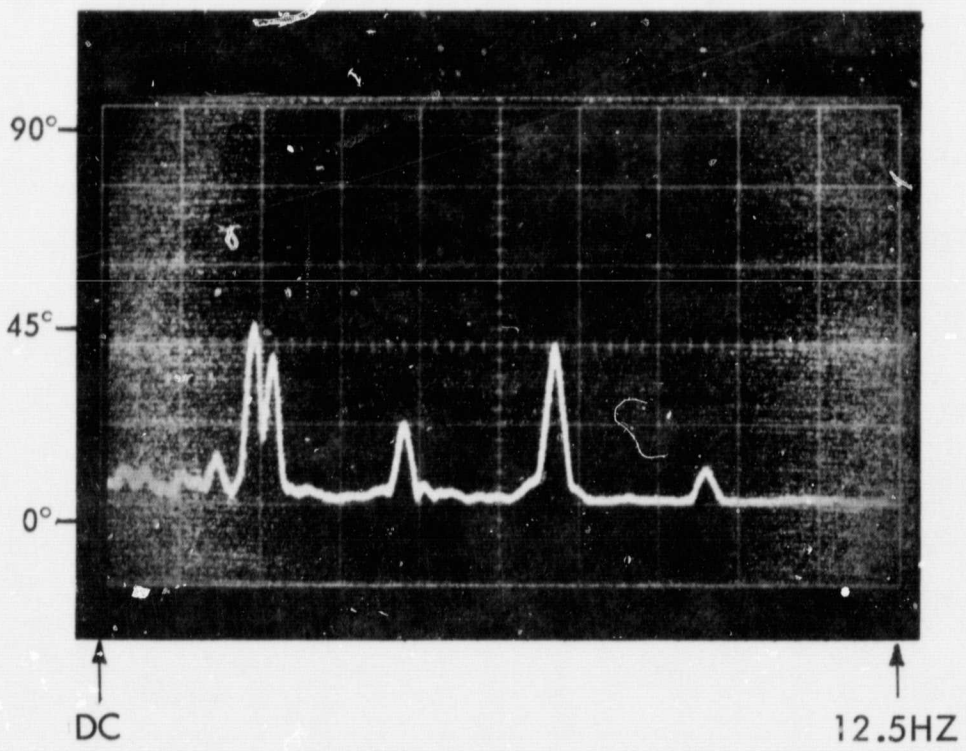

TYPICAL FREQUENCY SPECTRUM OF THE RELATIVE PHASE

Figure 19. RELAY II Experiment, 180' Antenna Spacing

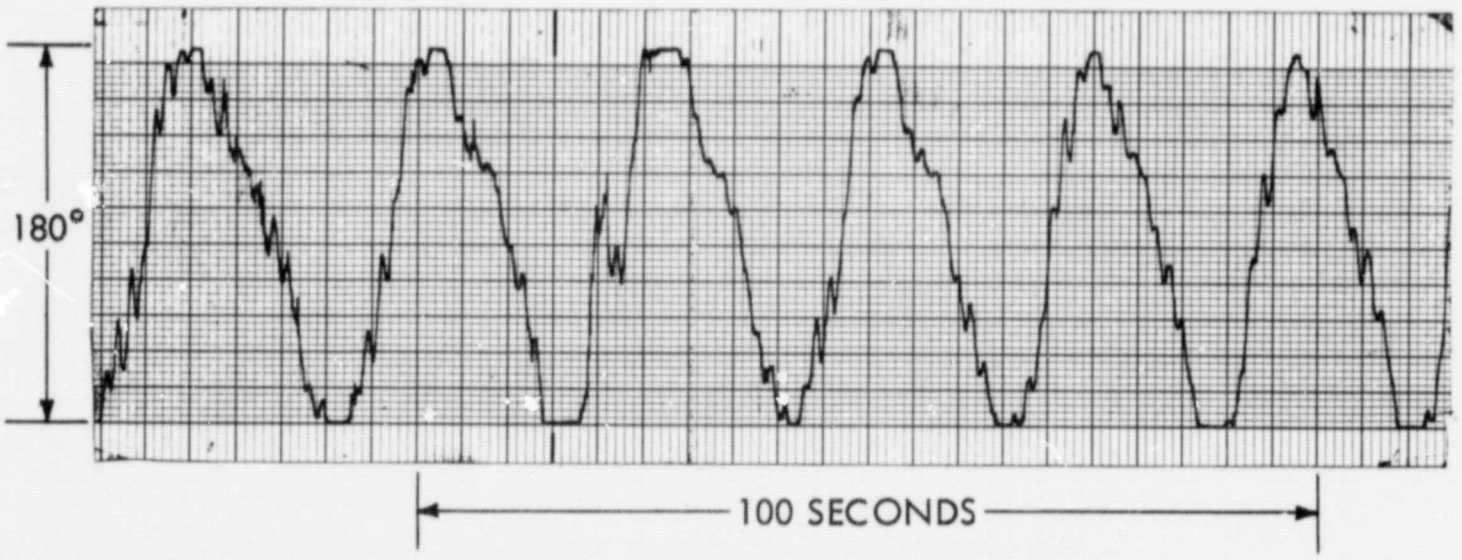

STRIP CHART RECORDING OF RELATIVE PHASE

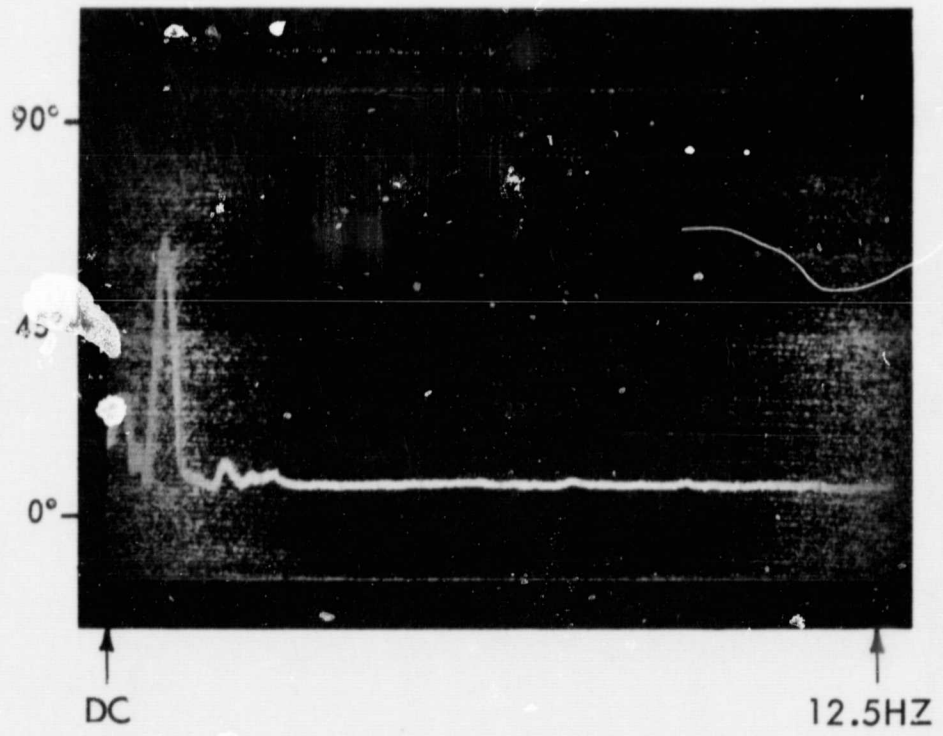

TYPICAL FREQUENCY SPECTRUM OF THE RELATIVE PHASE

Figure 20. ESSA-6 Experiment, 180' Antenna Spacing

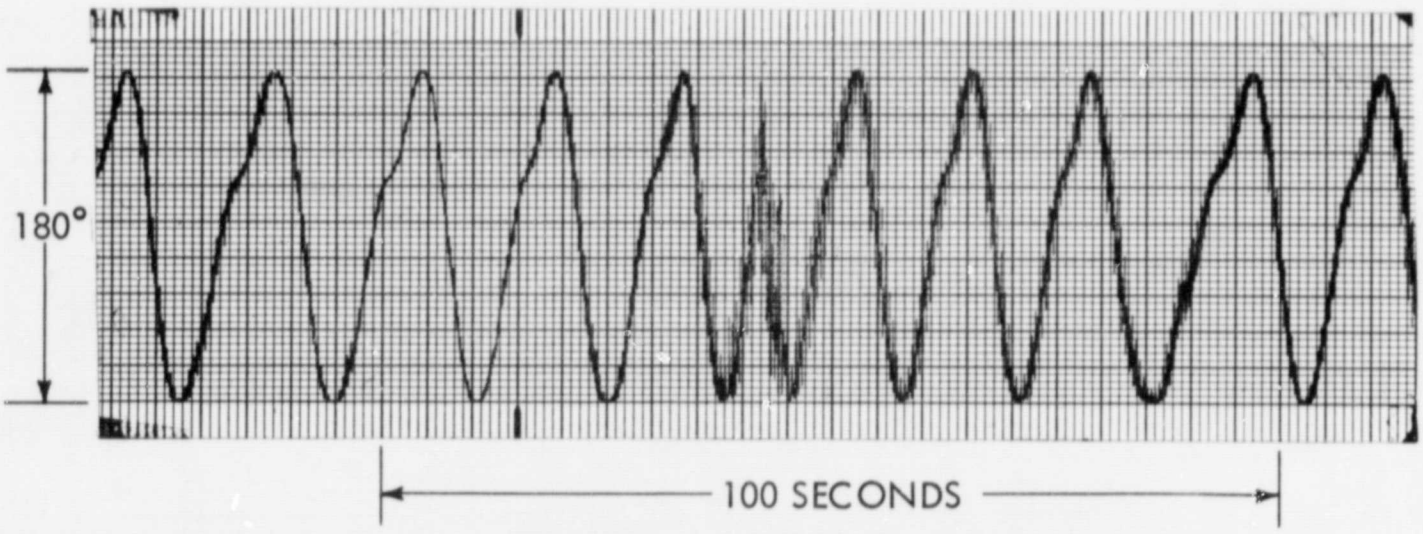

STRIP CHART RECORDING OF RELATIVE PHASE

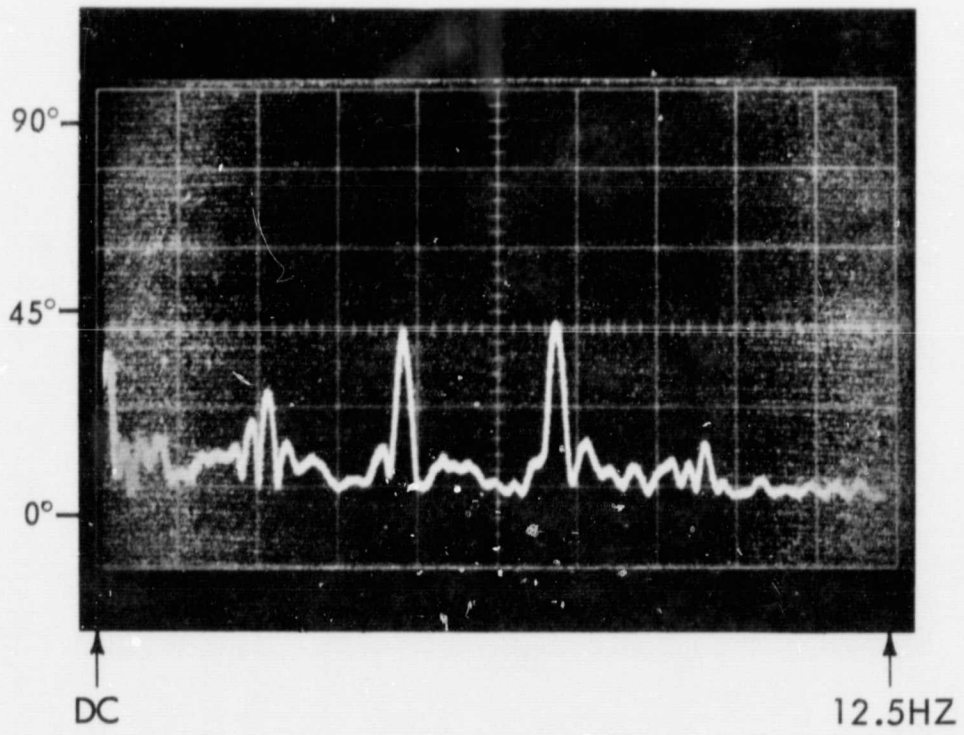

TYPICAL FREQUENCY SPECTRUM OF THE RELATIVE PHASE

Figure 21. RELAY II Experiment, 440' Antenna Spacing

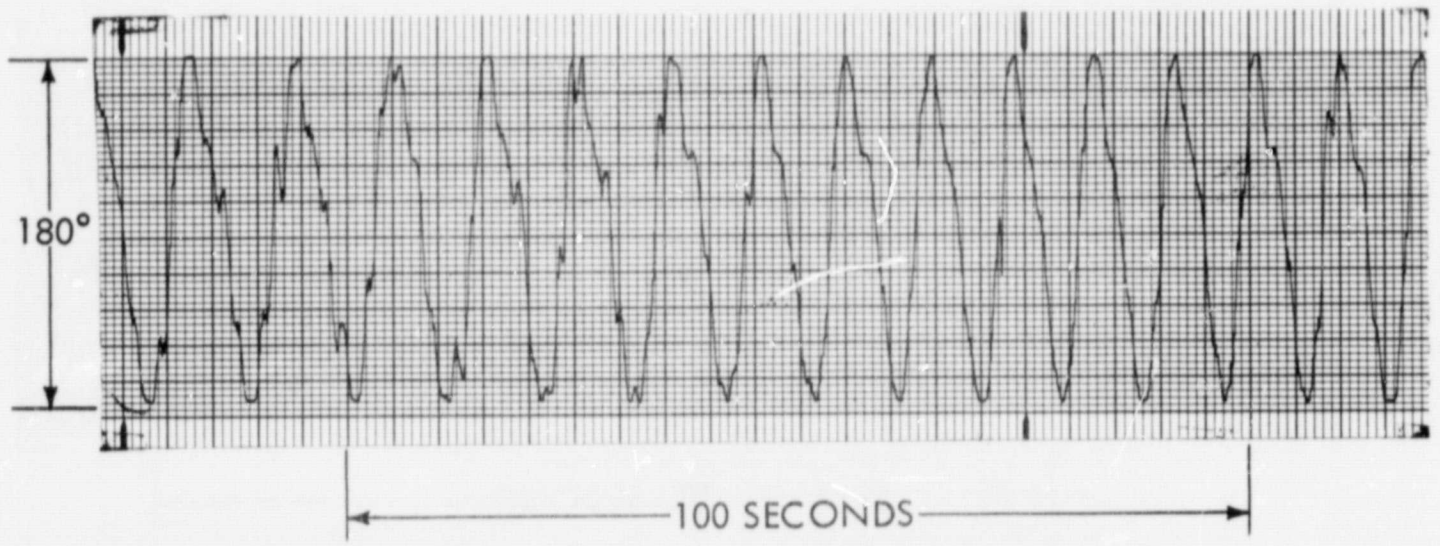

STRIP CHART RECORDING OF RELATIVE PHASE

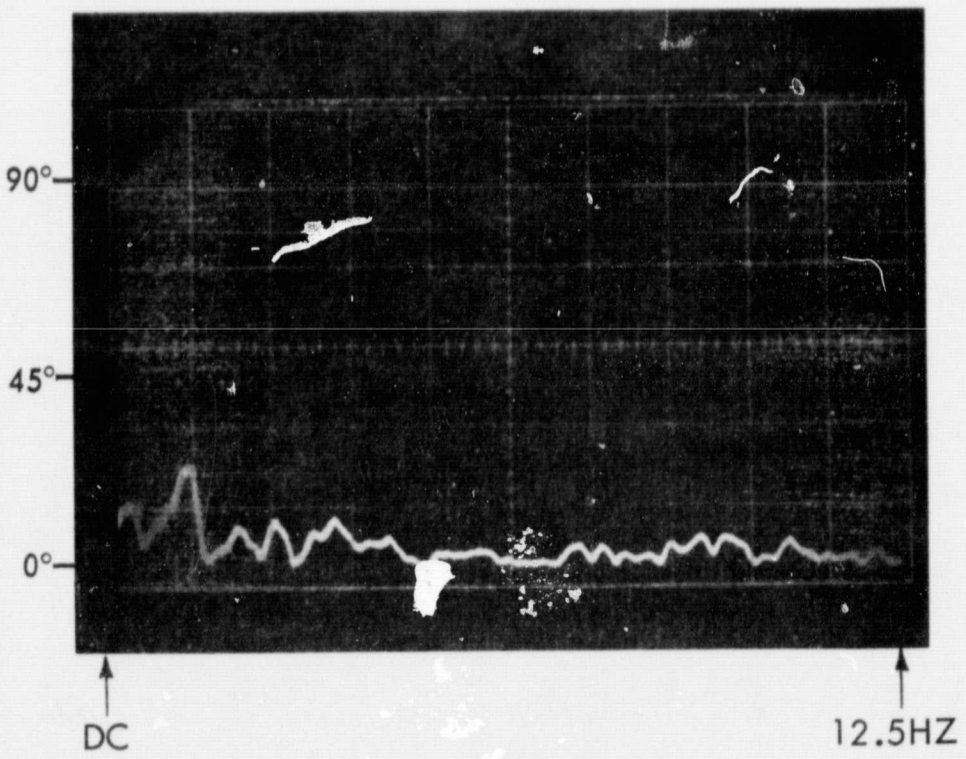

TYPICAL FREQUENCY SPECTRUM OF THE RELATIVE PHASE

Figure 22. ESSA-3 Experiment, 440' Antenna Spacing

but were considerably less significant. The spectra of the relative phase (Figures 19 through 24) represent an eight second average of the data recorded on magnetic tape. Although these photographs indicate the spectra for only a few seconds of an entire pass, care was taken in their choice to make them as representative of the actual data as possible.

An antenna spacing of 900 feet resulted in a small increase in the random components of the phase spectra for both RELAY II and ESSA satellites. The change from 440 to 900' spacing was considerably less significant than from 180 to 440'. Figures 23 and 24 represent two experiments with RELAY II which indicate substantial differences for a given antenna spacing. Figure 24 represents data at 900' spacing, but the difference in measured relative phase from that of Figure 23 is clearly seen. This phenomenon has occurred at all spacings and attempts to correlate the spectral characteristics with satellite trajectory and local weather conditions have been unsuccessful.

The strip chart segments associated with each spectrum represent typical relative phase measurements corresponding to that experiment. The slowly varying components are due to changing time-of-arrival delay between antennas, and the rate of variation is a function of the satellite and the antenna spacing. The occasional superposition of higher frequency components on the recordings for RELAY II are due to periods of signal fading in one of the antennas. Frequency spectra of this data indicate that these periods of increased activity are random and are not composed of predictable components. Spectral analysis beyond 12.5 Hz was performed. However, since no repetitious components were present and since the random components were similar to those for spectra below 12.5 Hz, the data is not presented here.

DISCUSSION

The results presented in this report are representative of the operational capability of an antenna combining system using the APDAR receiver as the coherent combiner. The data from ATS-C experiments shows that better than 1.75 dB SNR improvement was measured only 50 percent of the time. However, detailed analysis of the data indicates that the receiver design goal of maintaining the SNR improvement within 0.5 dB of the theoretical maximum was achieved 87% of the time. The remaining 13% of the data represented cases for which the input SNRs were more than 3.0 dB different. For these input conditions the APDAR receiver has been found, from calibration tests, to be unable to meet the design goal.

On the basis of the results from the VHF program, a SNR improvement within 0.5 dB of theoretical expectations can practically be expected in situations

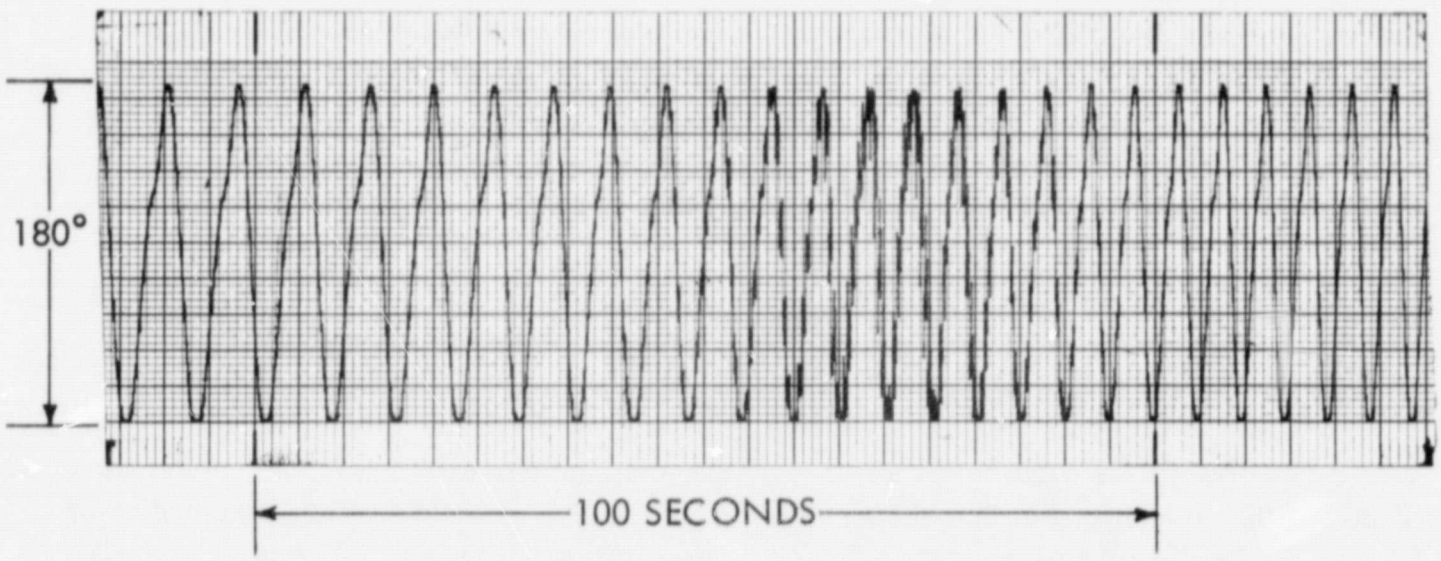

STRIP CHART RECORDING OF RELATIVE PHASE

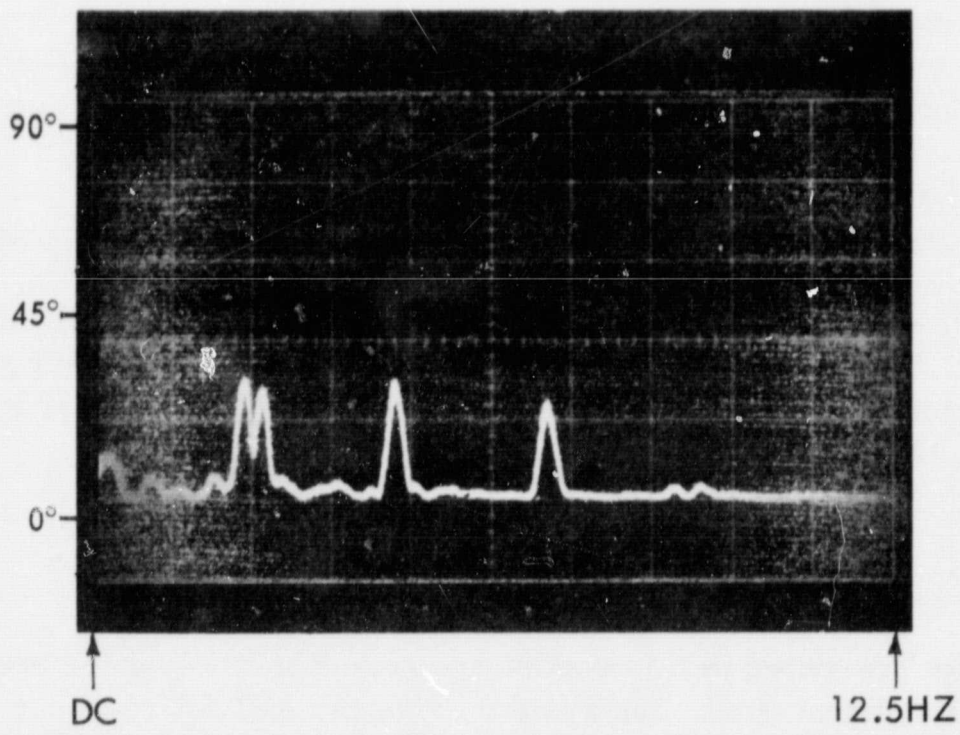

TYPICAL FREQUENCY SPECTRUM OF THE RELATIVE PHASE

Figure 23. RELAY II Experiment, 900' Antenna Spacing

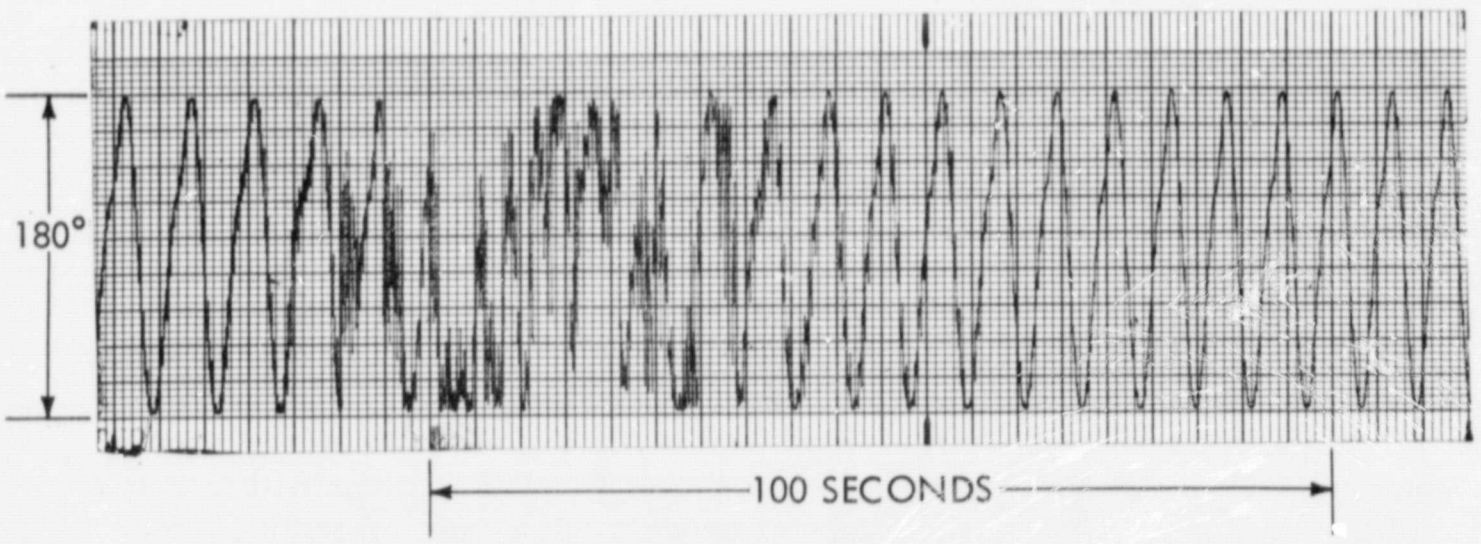

STRIP CHART RECORDING OF RELATIVE PHASE

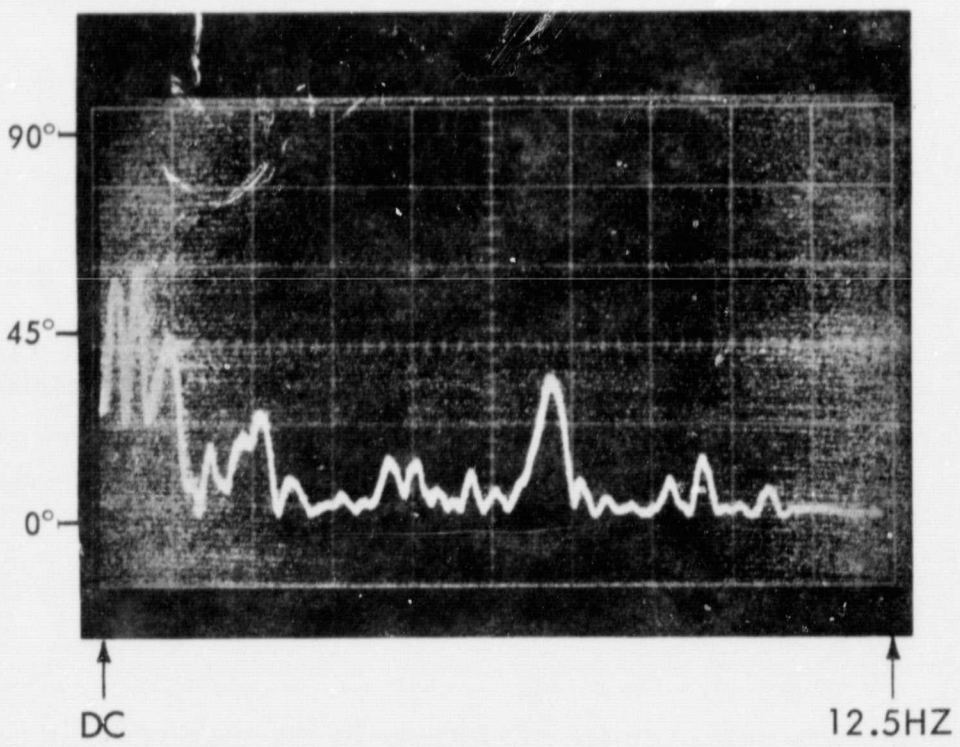

TYPICAL FREQUENCY SPECTRUM OF THE RELATIVE PHASE

Figure 24. RELAY II Experiment, 900' Antenna Spacing

where the array elements maintain their individual SNRs within 3.0 dB of each other. This condition was met for 87% of the data during ATS-C experiments and is, therefore, a realistic figure. When the two array elements provide approximately equal SNRs, the resulting SNR improvement will then be better than 2.5 dB.

The rapid degradation of improvement with differing input SNRs is a deficiency in the weighting process of the receiver and is undesirable in applications where large differential fading is a common occurrence. The SNR measurement program was substantially limited in satellite experiments by the large sampling periods required in the detection circuits. Modifications will be made to eliminate this requirement in future programs, and a wider breadth of tests will then be made practical.

Analysis of the detection circuits has indicated that the major error contribution in the data will be the result of inaccurate measurements of S + N. Estimates of this type of error contribution are easily calculated and are directly related to the SNR. As a result of this analysis, the data presented in this report is considered accurate to better than 0.2 dB. This accuracy refers to relative measurements between the three channels and does not refer to absolute values.

The random components of the relative phase measurements showed distinct changes with spacing, the major variations occurring between spacings of 180 and 440'. These random components represent phase front distortion of the incoming signal and its characteristics have been seen to vary substantially with time. The repetitive components found in RELAY II experiments indicate that the spin rate of a satellite can place an added requirement on the receiver in performing the coherence operation.

ACKNOWLEDGMENTS

The author wishes to acknowledge the efforts of Thomas W. Tunney and John E. Fuchs in the measurement and data reduction phases of the program. The assistance of Fred A. Wulff of the Data Processing Branch, Information Processing Division in performing spectral analysis of the relative phase data is also acknowledged.

REFERENCES

1. Investigation and Study of a Multi-Aperture Antenna System, Final Report. Contract NAS5-3472, Electronic Communications, Inc., April 1964.

2. Brennan, D. G.: Linear Diversity Combining Techniques, IEEE Proceedings, Vol. 47, June 1959.

3. An Adaptively Phased, Four-Element Array of Thirty-Foot Parabolic Reflectors for Passive (ECHO) Communication Systems. Contract AF 30(602)-2166, the Ohio State University Research Foundation, Nov. 30, 1964.

4. Taylor, R. E.: Satellite Tracking Simultaneous-Lobing Monopulse Receiving System with Polarization Diversity Capability, IEEE Transactions on Aerospace and Electronic Systems, Vol. AES-3, July 1967.

5. Viterbi, A. J.: Principles of Coherent Communication, McGraw-Hill Co., Inc., 1966.

6. Taylor, R. E.: Advanced Polarization Diversity Autotrack Receiver (APDAR) 136 MC Satellite Tracking Evaluation Tests, GSFC X-523-66-42, Feb. 1, 1966.

7. Gardner, F. M.: Phaselock Techniques, John Wiley & Sons, Inc., 1966.

APPENDIX A

As stated in the Time Delay System section of this report, the information signal to noise ratio improvement will be a function of the uncorrected time of arrival delay. Assuming a two-element array with equal SNRs in each channel, Figure A1 gives the maximum loss in SNR as a function of the relative phase of the information signals. The loss figures indicated are relative to an output SNR 3 dB above that of the input channels. The curve in Figure A1 is given by

$$\text{Power Loss} = \cos^2\left(\frac{\psi}{2}\right)$$

where

$$\psi = 2\pi \, Tf \tag{A1}$$

T = time delay

f = modulating frequency

This relation assumes equal S and N levels in each input channel. Such a condition corresponds to the worst case and the relation is derived below for an assumed input signal amplitude of unity:

$$\begin{aligned} S_1 &= \sin(\omega t) \\ S_2 &= \sin(\omega t - \psi) \\ S_1 + S_2 &= 2\cos\left(\frac{\psi}{2}\right)\sin\left(\omega t - \frac{\psi}{2}\right) \\ (S_1 + S_2)^2 &= 4\cos^2\left(\frac{\psi}{2}\right)\sin^2\left(\omega t - \frac{\psi}{2}\right) \end{aligned} \tag{A2}$$

Now since the input signal power levels are equal and independent of their respective phase, Equation A2 can be written as:

$$(S_1 + S_2)^2 = 4\cos^2\left(\frac{\psi}{2}\right) S_{1N}^2$$

The input noise contributions are incoherent and therefore add as their power in the combiner, giving:

$$N_1^2 + N_2^2 = 2\,N_{1N}^2$$

where

$$N_{1N} = N_1 = N_2$$

The SNR of the combined output channel is therefore:

$$SNR_c = \frac{(S_1 + S_2)^2}{N_1^2 + N_2^2} = \frac{4\cos^2\left(\frac{\psi}{2}\right) S_{1N}^2}{2\,N_{1N}^2}$$

$$SNR_c = 2\cos^2\left(\frac{\psi}{2}\right) [SNR]_{1N}$$

As described in this report, the time delay system developed for the antenna combining project was digitally variable in 90.9 nanosecond steps. Assuming an overlap of nine nanoseconds in the delay control unit, the maximum delay experienced by the system is 50 nanoseconds for any antenna spacing up to 2860 feet. Referring to Equation A1, T is therefore fixed at 50 nanoseconds and the maximum power loss is therefore only a function of frequency. For the system described above, the maximum signal loss is given in Figure A2 as a function of the modulating frequency.

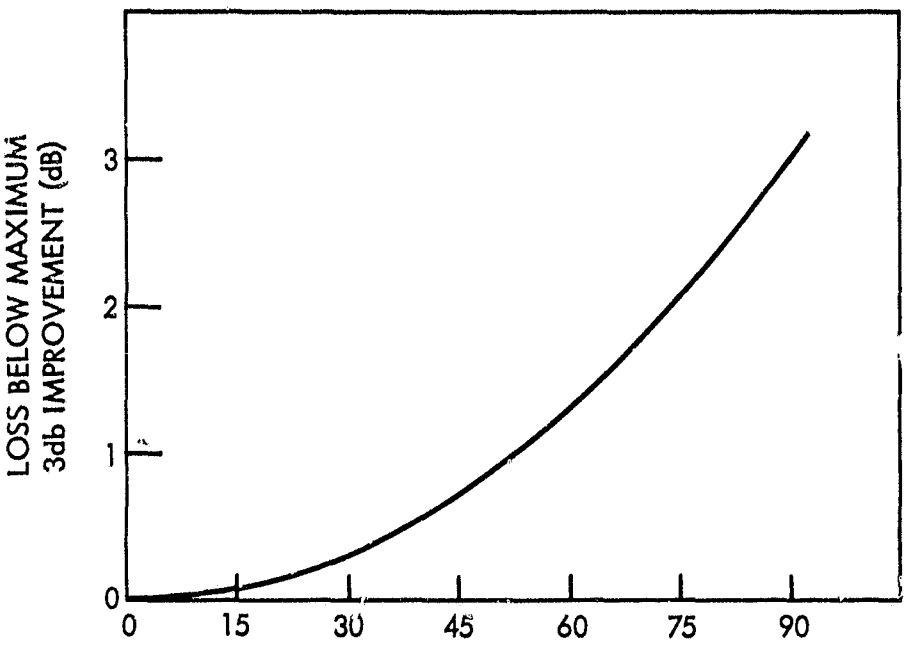

Figure A1. Maximum Signal Loss Versus Phase Difference

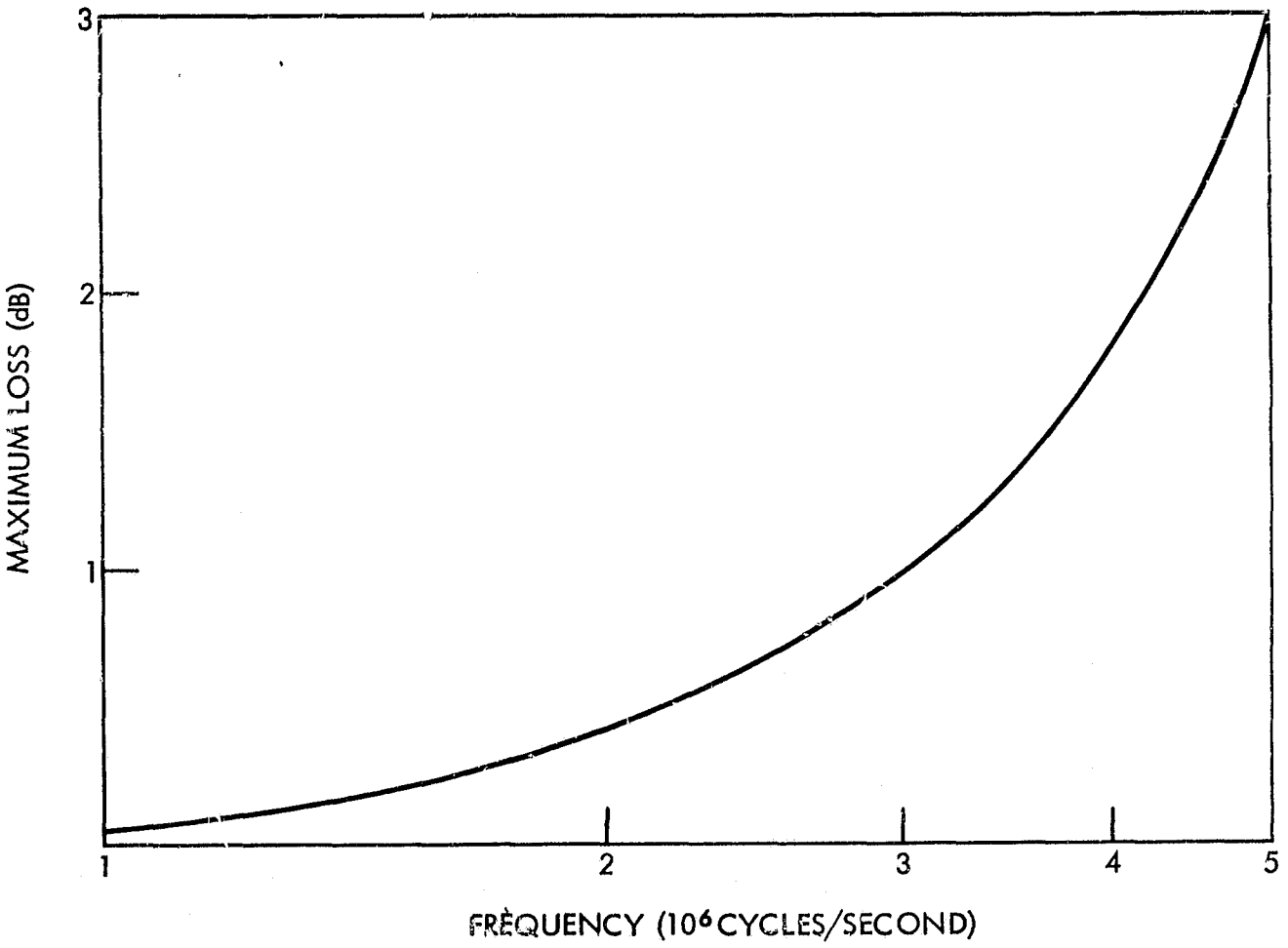

Figure A2. Maximum Signal Loss Versus Frequency

APPENDIX B

As described by Gardner[1] the signal power and noise power out of a bandpass limiter are a function of the input signal-to-noise ratio. The relation is given approximately as:

$$S \cong \frac{2L^2}{\pi}\left[\frac{4(SNR)_i/\pi}{4/\pi + (SNR)_i}\right]$$

$$N \cong \frac{2L^2}{\pi}\left[\frac{4/\pi}{1 + 2(SNR)_i}\right]$$

where L is related to the peak output voltage of the limiter. The two equations can be combined into one describing the output SNR as a function of the input SNR:

$$SNR_0 \cong (SNR)_i \frac{1 + 2(SNR)_i}{4/\pi + (SNR)_i}$$

The relationship is given graphically in Figure B1.

[1]Reference 7, pp. 55-58

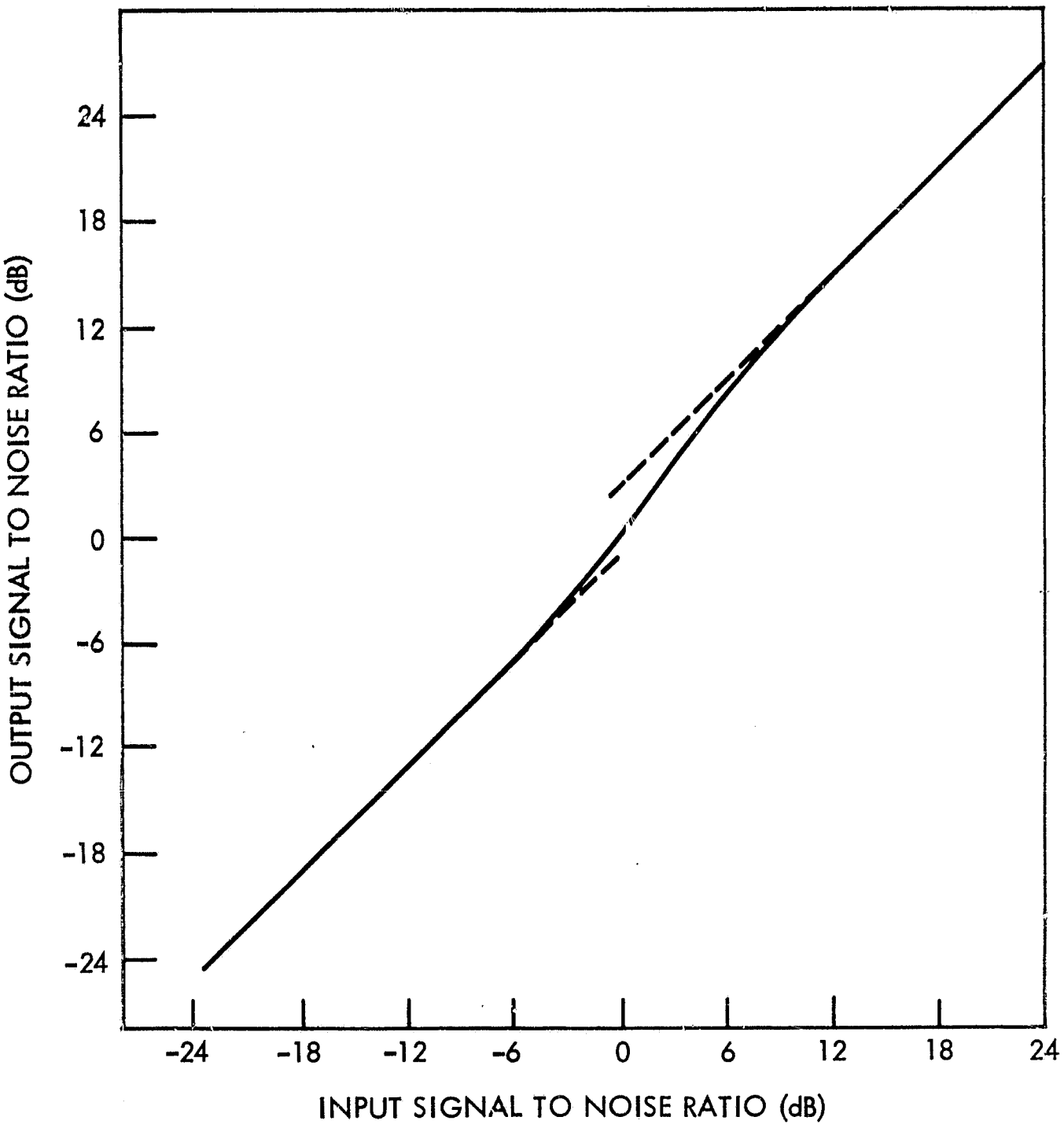

Figure B1. SNR Characteristics of a Bandpass Limiter

APPENDIX C

The weighting process in the APDAR receiver is an important consideration and an explanation of its significance will be given here. The simplified system block diagram given in Figure C1 shows the components affecting the weighting process. The preamplifier in the figure is broken into noise figure and gain sections. The gain figures of G_1 and G_2 represent net gain from the input of the preamplifier to the input of the receiver and therefore includes cable losses. The noise figure contributions shown represent the noise figure of the entire system channel referred to in the input of the preamplifier.

The APDAR receiver is divided into three stages: RF amplifier section, IF amplifier section, and combiner section. The RF amplifiers have constant gain characteristics which are adjustable. The IF amplifiers are actively gain controlled by the AGC outputs of the coherent detectors. The output signal levels from the IF amplifiers are thereby maintained constant. The automatic gain control signal therefore represents a measure of the output signal from the RF amplifiers. The combiner in turn accepts the AGC output as proportional to the signal level into the preamplifiers for that channel. The process is correct to within the gain differences of the system prior to the IF amplifiers. The total signal and noise power arriving at the IF amplifiers is given by

$$G_1 G_3 (S_1^2 + N_1^2 + N_{F1}^2) \tag{C1}$$

for channel 1, and by

$$G_2 G_4 (S_2^2 + N_2^2 + N_{F2}^2) \tag{C2}$$

for channel 2. The gain products in each channel must be identical for the combiner to weight the signals properly.

The combiner assumes that the AGC or S level is representative of the SNR in a given channel. Expressions C1 and C2 indicate that the assumption will be in error by the difference in received noise levels N_1 and N_2 and also by the difference in channel noise figure contributions N_{F1} and N_{F2}. Care was taken in the experimental phase of the program described in this report to match the noise figures of the sum channel preamplifiers, essentially eliminating this type of error contribution. The input noise levels are unpredictable and will depend

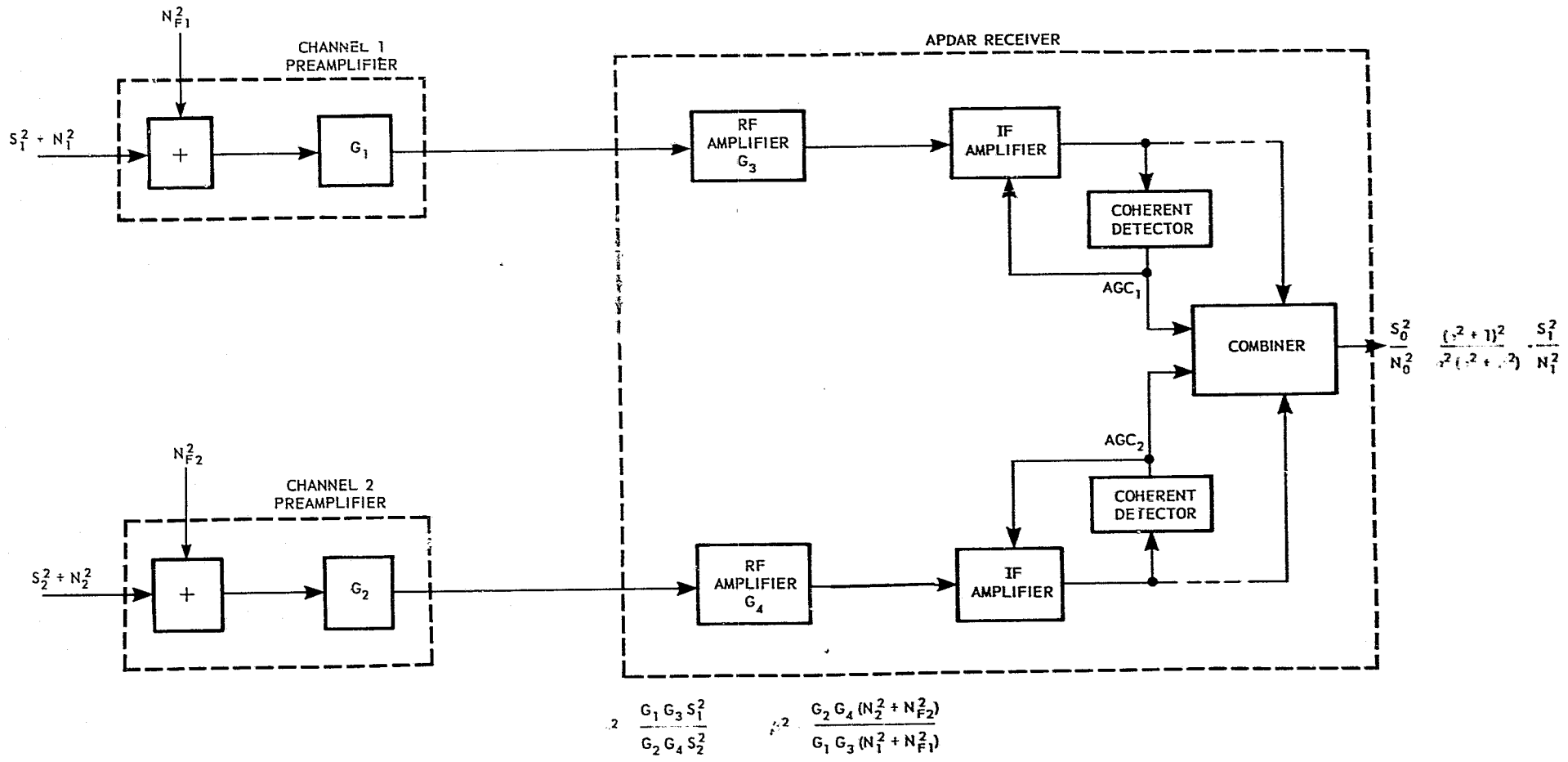

Figure C1. System Model for Studying APDAR AGC Weighting Process

on contributions from numerous sources. The results of the measurement program will in effect determine the significance of this error and the effectiveness of AGC weighting in space diversity applications.

Unequal channel gain products given in expressions C1 and C2 will also lead to inaccurate weighting. However, compensation for gain differences in the preamplifiers can be made in the RF amplifiers of the receiver. The effect of not performing this adjustment can be easily calculated. Assuming for this analysis that the combiner weights only channel 1 in relation to channel 2 the expressions can be written:

$$S_0^2 = B (\propto S_1 + S_2)^2 \tag{C3}$$

$$N_0^2 = B \left[\propto^2 (N_1^2 + N_{F1}^2) + N_2^2 + N_{F2}^2\right] \tag{C4}$$

where S_0^2 and N_0^2 represent the output signal and noise power levels from the combiner with B a constant of channel 2. The factor $\propto$ is given by

$$\propto^2 = \frac{G_1 G_3 S_1^2}{G_2 G_4 S_2^2}$$

and contains the relative gain products of the two channels. Expressions C3 and C4 can then be written in terms of channel 1 signal and noise only:

$$S_0^2 = S_1^2 \left(\propto + \frac{1}{\propto}\right)^2 = S_1^2 \left(\frac{\propto^2 + 1}{\propto}\right)^2 \tag{C5}$$

$$N_0^2 = (N_1^2 + N_{F1}^2) (\propto^2 + \beta^2) \tag{C6}$$

where

$$\beta^2 = \frac{G_2 G_4 (N_2^2 + N_{F2}^2)}{G_1 G_3 (N_1^2 + N_{F1}^2)}$$

the effect of gain differences can be seen readily from an example. For the conditions

$$S_1 = S_2$$

$$N_1 = N_2$$

$$N_{F1} = N_{F2}$$

and with a gain difference of 3.0 dB between channels

$$\frac{G_1\ G_3}{G_2\ G_4} = 1.414$$

giving

$$\alpha = 1.414$$

$$\beta = 0.708$$

The output signal-to-noise ratio can now be calculated using expressions C5 and C6:

$$\frac{S_0^2}{N_0^2} = \frac{(\alpha^2 + 1)^2}{\alpha^2\ (\alpha^2 + \beta^2)} \cdot \frac{S_1^2}{N_1^2}$$

$$\frac{S_0^2}{N_0^2} = 1.8 \left(\frac{S_1^2}{N_1^2} \right)$$

where the result is 2.55 dB improvement over channel 1. Since the input SNRs were equal the improvement should have been 3.0 dB.

The analysis made above to show the characteristics of the present system is valid for any diversity receiver using AGC weighting in the combiner. The differential gain influence is essentially eliminated by properly compensating for it in the receiver RF amplifier stage. The channel noise figures are matched by carefully selecting the preamplifiers for the monopulse sum channels. The effect of differential noise reception by the antenna, however, cannot be eliminated in the present receiver and true SNR weighting must be used for optimum performance. The experimental program was designed to determine the effectiveness of the APDAR receiver and AGC weighting in operational space diversity applications.

The SNR measurements made in this program were measured at the combiner input and output terminals and were not affected by the AGC limitations of the receiver. Therefore, the comparison made between recorded and theoretical data later in the report does reflect any loss in SNR improvement that may have occurred.